Impacts of bromine and iodine chemistry on tropospheric OH and HO_2: Comparing observations with box and global model perspectives

Daniel Stone,[1] Tomás Sherwen,[2] Mathew J. Evans,[2,3] Stewart Vaughan,[1] Trevor Ingham,[1,4] Lisa K. Whalley,[1,4] Peter M. Edwards,[2] Katie A. Read,[2,3] James D. Lee,[2,3] Sarah J. Moller,[2,3] Lucy J. Carpenter, [2,3] Alastair C. Lewis, [2,3] Dwayne E. Heard[1,4]

[1] School of Chemistry, University of Leeds, Leeds, UK
[2] Wolfson Atmospheric Chemistry Laboratories, Department of Chemistry, University of York, York, UK
[3] National Centre for Atmospheric Science, University of York, York, UK
[4] National Centre for Atmospheric Science, University of Leeds, Leeds, UK

Abstract

The chemistry of the halogen species bromine and iodine has a range of impacts on tropospheric composition, and can affect oxidising capacity in a number of ways. However, recent studies disagree on the overall sign of the impacts of halogens on the oxidising capacity of the troposphere. We present simulations of OH and HO_2 radicals for comparison with observations made in the remote tropical ocean boundary layer during the Seasonal Oxidant Study at the Cape Verde Atmospheric Observatory in 2009. We use both a constrained box model, using detailed chemistry derived from the Master Chemical Mechanism (v3.2), and the three-dimensional global chemistry transport model GEOS-Chem. Both model approaches reproduce the diurnal trends in OH and HO_2. Absolute observed concentrations are well reproduced by the box model but are overpredicted by the global model, potentially owing to incomplete consideration of oceanic sourced radical sinks. The two models, however, differ in the impacts of halogen chemistry. In the box model, halogen chemistry acts to increase OH concentrations (by 9.8 % at midday at Cape Verde), while the global model exhibits a small increase in OH at Cape Verde (by 0.6 % at midday) but overall shows a decrease in the global annual mass weighted mean OH of 4.5 %. These differences reflect the variety of timescales through which the halogens impact the chemical system. On short timescales, photolysis of HOBr and HOI, produced by reactions of HO_2 with BrO and IO, respectively, increases the OH concentration. On longer timescales, halogen catalysed ozone destruction cycles lead to lower primary production of OH radicals through ozone photolysis, and thus to lower OH concentrations. The global model includes more of the longer timescale responses than the constrained box model and overall the global impact of the longer timescale response (reduced primary production due to lower O_3 concentrations) overwhelms the shorter timescale response (enhanced cycling from HO_2 to OH), and thus the global OH concentration decreases. The Earth system contains many such responses on a large range of timescales. This work highlights the care that needs to be taken to understand the full impact of any one process on the system as a whole.

Introduction

Halogen chemistry in the troposphere influences budgets of O_3, HO_x (OH and HO_2), NO_x (NO and NO_2) (von Glasow et al., 2004; Saiz-Lopez and von Glasow, 2012; Simpson et al., 2015, Schmidt et al., 2016; Sherwen et al., 2016a; Sherwen et al., 2016b), affects the oxidation state of atmospheric mercury (Holmes et al., 2006; Holmes et al., 2010), and impacts aerosol formation (Hoffmann et al., 2001; O'Dowd et al., 2002; McFiggans et al., 2004; McFiggans et al., 2010; Mahajan et al., 2011; Sherwen et al., 2016c).

The production of bromine and iodine atoms in the marine boundary layer (MBL) following emissions of organohalogen compounds and the inorganic compounds I_2 and HOI has been shown to result in considerable destruction of tropospheric ozone (Read et al., 2008), leading to the production of bromine monoxide (BrO) and iodine monoxide (IO) radicals. Observations of BrO and IO radicals within the MBL have demonstrated widespread impacts on atmospheric composition and chemistry (Alicke et al., 1999; Sander et al., 2003; Leser et al., 2003; Saiz-Lopez and Plane, 2004; Saiz-Lopez et al., 2004; Peters et al., 2005; Saiz-Lopez et al., 2006; Whalley et al., 2007; Mahajan et al., 2010a; Commane et al., 2011; Dix et al., 2013; Gomez Martin et al., 2013; Le Breton et al., 2017), including significant effects on HO_x concentrations and on the HO_2:OH ratio in coastal and marine locations (Bloss et al., 2005a; Sommariva et al., 2006; Bloss et al., 2007; Bloss et al., 2010; Kanaya et al., 2007; Whalley et al., 2010).

The role of halogens in HO_x chemistry was demonstrated during the NAMBLEX campaign in Mace Head, Ireland, (Heard et al., 2006), following several studies which attributed box model overestimates of HO_2 observations in marine environments to unmeasured halogen monoxides (Carslaw et al., 1999; Carslaw et al., 2002; Kanaya et al., 2001; Kanaya et al., 2002; Kanaya et al., 2007). Simultaneous measurements of OH and HO_2 by laser-induced fluorescence (LIF) (Bloss et al., 2005a; Smith et al., 2006) and halogen species by a combination of DOAS (for BrO or IO, OIO and I_2) (Saiz-Lopez et al., 2006) and broadband cavity ringdown spectroscopy (BBCRDS) (for OIO and I_2) (Bitter et al., 2005) during NAMBLEX enabled box model calculations to fully explore the impacts of halogens on the local composition. A box model without halogen chemistry was able to reproduce the NAMBLEX OH observations to within 25 %, but HO_2 observations were overestimated by up to a factor of 2 (Sommariva et al., 2006). The introduction of halogen chemistry, using DOAS measurements of BrO and IO (Saiz-Lopez et al., 2006) to constrain the model, increased the modelled OH concentrations by up to 15 % and decreased HO_2 by up to 30 % owing to reactions of HO_2 with XO radicals to form HOX which subsequently photolysed to X + OH (Sommariva et al., 2006). Bloss et al., (2005a) indicated that up to 40 % of the instantaneous HO_2 loss could be attributed to HO_2 + IO, and that photolysis of HOI was responsible for 15 % of the noontime OH production.

The impacts of halogen chemistry on HO_x radicals at a site representative of the open ocean have been investigated at the Cape Verde Atmospheric Observatory (CVAO). Measurements of halogen monoxides (Mahajan et al., 2010a) at the site have been shown to have significant impacts on local ozone concentrations, notably in the magnitude of the daily cycle (Read et al., 2008), and have been used to constrain box model calculations used to explore observations of OH and HO_2 made during the RHaMBLe campaign in 2007 (Whalley et al., 2010). The model calculations showed generally good comparisons with the observed OH and HO_2 concentrations, apart from a period characterised by unusually high concentrations of HCHO. Compared to a model run in which halogen chemistry was absent, bromine and iodine chemistry led to a 9 % increase in the modelled OH concentration (Whalley et al., 2010). Owing to the dominance of the tropics in global methane oxidation (Bloss et al., 2005b), such an impact of halogens on OH could have significant consequences for estimates of global methane lifetimes, and on our understanding of the impacts of halogen chemistry on climate change.

In general, observationally constrained box model simulations suggest that halogens in the troposphere will increase OH concentrations, primarily because of a change in the HO_2 to OH ratio occurring as a result of reactions of halogen oxides (XO) with HO_2 to produce a hypohalous acid (HOX) which photolyses to give an OH radical and a halogen atom (Kanaya et al., 2002; Bloss et al., 2005a; Kanaya et al., 2007; Sommariva et al., 2006; Sommariva et al., 2007; Whalley et al., 2010). Other impacts on the HO_x photochemical system are observed (impacts from changes to NO_x chemistry etc.) but these are minor and overall the general conclusion is that the halogen chemistry tends to increase the OH concentration and thus the oxidising capacity of the atmosphere.

However, the observationally constrained studies are typically concerned with processes occurring at the surface, and in a single location. The role of halogen chemistry in the troposphere as a whole is more uncertain, particularly in the free troposphere and on a global scale (Saiz-Lopez and von Glasow, 2012; Simpson et al., 2015). Inclusion of bromine chemistry in the three-dimensional (3D) chemistry transport model (CTM) MATCH-HPIC resulted in decreases in tropospheric ozone concentrations of ~18 % over widespread areas, with regional decreases of up to 40 % (von Glasow et al., 2004). Increases of more than 20 % were found for OH in the free troposphere, but, globally, changes to OH were dominated by decreases in OH in the tropics owing to a reduction in primary production from O_3 photolysis, leading to a decrease of 1-2 % in the global mean OH concentration (von Glasow et al., 2004).

Significant decreases in tropospheric ozone (up to 30% at high latitude spring) were also reported for the pTOMCAT model on inclusion of bromine chemistry (Yang et al., 2005). The CAM-Chem global chemistry-climate model has shown an approximate 10 % decrease in global mean tropospheric ozone concentration on

incorporation of lower bromine emissions (Saiz-Lopez et al., 2012), while the GEOS-Chem CTM displays a global decrease of 6.5 % (Parrella et al., 2012). The GEOS-Chem model indicated that bromine-catalysed loss of ozone is limited by the rate of production of HOBr, and that HO_2 + BrO is responsible for over 95 % of the global tropospheric HOBr production. While HOBr can act as a source of OH on photolysis, the changes to O_3 and NO_x resulting from the inclusion of bromine chemistry in GEOS-Chem led to a 4 % decrease overall in the global annual mean OH (Parrella et al., 2012).

Vertically resolved airborne measurements of IO radicals in the free troposphere over the Pacific Ocean have also demonstrated a role for iodine chemistry throughout the free troposphere, with IO observed at a mixing ratio of ~0.1 ppt in the free troposphere and found to be present in both recent deep convective outflow and aged free tropospheric air (Dix et al., 2013). Model simulations to investigate iodine-driven ozone destruction throughout the troposphere indicated that only 34 % of the total iodine-driven ozone loss occurs within the marine boundary layer, with 40 % occurring in a transition layer and 26 % in the free troposphere (Dix et al., 2013).

The CAM-Chem and GEOS-Chem models have also been updated to encompass iodine chemistry, with results from CAM-Chem showing iodine chemistry to be responsible for 17-27 % of the ozone loss in the tropical MBL and 11-27 % of the ozone loss in the marine upper troposphere (Saiz-Lopez et al., 2014). The GEOS-Chem model also showed iodine chemistry to be responsible for significant ozone destruction throughout the troposphere (Sherwen et al., 2016a; Sherwen et al., 2016b; Sherwen et al., 2017). The GEOS-Chem simulations, which incorporate chlorine, bromine and iodine chemistry, show a reduction in global tropospheric ozone concentration of 18.6 %, compared to simulations with no halogen chemistry, a reduction in the global mean OH of 8.2 % to a concentration of 1.28×10^6 cm^{-3} and a resulting increase in global methane lifetime of 10.8 % to 8.28 years (Sherwen et al., 2016b).

There is thus a discrepancy between box and global models as to the impact of halogen chemistry on OH concentrations in the troposphere. Box models suggesting that OH radical concentrations should increase and thus that halogens tend to increase the oxidising capacity, whereas the global models tend to suggest the opposite.

In this work, we use both a detailed chemical box model approach and a global chemistry-transport model to investigate the local and global impacts of halogen chemistry on HO_x radical concentrations. We focus on seasonal HO_x observations available from the Cape Verde Atmospheric Observatory (Vaughan et al., 2012). We first provide a summary of the measurement site and the observations, followed by details of the two models used

in this study. We then evaluate the impact of halogens on the concentrations of oxidants in the two modelling frameworks and consider the impact of halogen chemistry on global oxidising capacity.

The Cape Verde Atmospheric Observatory

The Cape Verde Atmospheric Observatory is situated on the north east coast of the island of Sao Vicente (16.848 ^{o}N, 24.871 ^{o}W), approximately 500 km off the west coast of Africa. The observatory is in a region of high marine biological production, and, for 95 % of the time, receives the prevailing northeasterly trade wind directly off the ocean (Read et al., 2008; Carpenter et al., 2010). Measurements at the observatory are considered to be representative of the open ocean, and CO, O_3, VOCs, NO_x and NO_y have been measured near-continuously at the observatory since October 2006 (Lee et al., 2009; Carpenter et al., 2010).

In 2007, the observatory was host to the RHaMBLe intensive field campaign, during which a number of additional measurements were made to complement the long-term measurements at the site (Lee et al., 2010), including LP-DOAS measurements of halogen species (Read et al., 2008; Mahajan et al., 2010a) and formaldehyde (Mahajan et al., 2010b), and LIF-FAGE measurements of OH and HO_2 (Whalley et al., 2010). The halogen monooxide radicals BrO and IO exhibited a 'top-hat' diurnal cycle (Vogt et al., 1999; Vogt et al., 1996; Read et al., 2008; Mahajan et al., 2010a) with essentially zero concentration in the hours of darkness and generally constant values of approximately 2.5 ppt BrO and 1.4 ppt IO during the day.

The RHaMBLe campaign was followed by the Seasonal Oxidants Study (SOS) in 2009, during which measurements of OH and HO_2 were conducted over three periods (Feb-March (SOS1), May-June (SOS2), and September (SOS3)), and are discussed in detail by Vaughan et al. (2012). We present here the results from a modelling study of the HO_x measurements made during SOS1 and SOS2, when supporting measurements are available, using both box and global model approaches. SOS3 is not considered in this work owing to a lack of supporting measurements.

Measurements of OH and HO_2 during the Seasonal Oxidant Study were made by laser-induced fluorescence (LIF) spectroscopy at low pressure using the fluorescence assay by gas expansion (FAGE) technique, and are described in detail by Vaughan et al. (2012). Briefly, ambient air is drawn into a fluorescence cell situated on the roof of a shipping container and maintained at pressures of ~ 2 Torr. The fluorescence cell has two excitation axes, with excess NO added at the second axis to titrate HO_2 to OH, enabling simultaneous detection of OH and HO_2. OH radicals in both excitation axes are excited by laser light at $\lambda \sim 308$ nm, generated by frequency tripling the output

of a solid state Nd:YAG pumped Ti:Sapphire laser system (Bloss et al., 2003). Channel photomultiplier tubes coupled to gated photon counters are used to detect the $A^2\Sigma^+ - X^2\Pi_i$ OH fluorescence signal at λ ~ 308 nm.

Calibration of the instrument is achieved by measurement of the fluorescence signal from known concentrations of OH and HO_2, produced by the photolysis of water vapour, and was performed over a range of conditions before, during and after the campaign. For OH, the 1 σ limit of detection (LOD) was in the range (2-11) × 10^5 cm^{-3} for a 5 min averaging period, while for HO_2 1 σ LOD was in the range (6-13) × 10^5 cm^{-3} for a 4 min averaging period. Uncertainties (2 σ) in the measurements of OH and HO_2 are ~32 % (Vaughan et al., 2012).

Potential interferences in HO_2 measurements arising from conversion of alkene- and aromatic-derived peroxy radicals to OH within the LIF detection cell, as described by Fuchs et al. (2011), are expected to be small for this work owing to relatively low concentrations of alkenes and aromatics at the Cape Verde observatory (Carpenter et al., 2010; Vaughan et al., 2012). Speciation of the peroxy radicals in the box model output (see Supplementary Material) shows that 87.4 % of the peroxy radicals are HO_2 and CH_3O_2, 6.5 % $CH_3C(O)O_2$ and 1.1 % $C_2H_5O_2$, all of which display no HO_2 interference in the laboratory (Whalley et al., 2013: Stone et al., 2014). Peroxy radicals derived from OH-initiated oxidation of ethene and propene ($HOC_2H_4O_2$ and $HOC_3H_6O_2$, respectively) were found to result in an interference signal for HO_2 in the laboratory (~40 % for the experimental configuration in this work) but each radical comprises only ~0.6 % of the total RO_2 in this work. Thus, model calculations reported here do not include representation of potential HO_2 interferences, although such phenomena may be important in other environments (see for example, Whalley et al., 2013; Stone et al., 2014).

Model Approaches

We interpret the observations using two different modeling frameworks. The first is an observationally constrained box model (DSMACC), the second is a global tropospheric chemistry transport model (GEOS-Chem).

Constrained Box Model

The Dynamically Simple Model of Atmospheric Chemical Complexity (DSMACC) is described in detail by Emmerson and Evans (2009) and Stone et al. (2010), and is a zero-dimensional model using the Kinetic Pre-Processor (KPP) (Sandu and Sander, 2006). In this work we use a chemistry scheme based on a subsection of the hydrocarbons (ethane, propane, *iso*-butane, *n*-butane, *iso*-pentane, *n*-pentane, hexane, ethene, propene, 1-butene, acetylene, isoprene, toluene, benzene, methanol, acetone, acetaldehyde and DMS) available from the Master Chemical Mechanism version 3.2 (MCM v3.2 http://mcm.leeds.ac.uk/MCM/home.htt) (Jenkin et al., 2003;

Saunders et al., 2003), with a halogen chemistry scheme described by Saiz-Lopez et al. (2006), Whalley et al. (2010) and Edwards et al. (2011). We also include the reaction between OH and CH_3O_2 (Bossolasco et al., 2014; Fittschen et al., 2014; Assaf et al., 2016; Yan et al., 2016), with a rate coefficient of 1.6×10^{-10} cm^3 s^{-1} (Assaf et al., 2016) and products HO_2 + CH_3O (Assaf et al., 2017), the impact of which on the HO_2:OH ratio and CH_3O_2 budget is described in the Supplementary Material. The total number of species in the model is ~1200, with ~5000 reactions. The full chemistry scheme used in the model is given in the Supplementary Data.

All measurements are merged onto a 10 minute timebase for input to the model and the model is run with constraints applied as discussed in our previous work (Stone et al., 2010; Stone et al., 2011; Stone et al., 2014). Concentrations of CH_4 and H_2 are kept constant at values of 1770 ppb (NOAA CMDL flask analysis, ftp://ftp.cmdl.noaa.gov/ccg/ch4/) and 550 ppb (Ehhalt and Rohrer, 2009; Novelli et al., 1999) respectively. Formaldehyde measurements were not available during the SOS and we thus use HCHO concentrations generated by the chemistry in the model, with the modelled HCHO concentrations in broad agreement with previous measurements at the observatory (Mahajan et al., 2010b). Table 1 shows a summary of the input parameters to the model.

Species	Mean	Median	Range
O_3 / ppb	33.8 ± 8.6	30.7	19.6 – 49.7
CO / ppb	102.3 ± 10.3	99.3	87.8 – 127.3
H_2O / ppm	20542.3 ± 2753.8	21290.0	16778.5 – 24909.2
NO / ppt	11.2 ± 10.6	9.0	0.06 – 96.2
Ethane / ppt	961.3 ± 289.4	864.0	625.4 – 1799.2
Propane / ppt	136.1 ± 87.05	111.8	20.2 – 521.5
***iso*-butane / ppt**	13.4 ± 9.8	11.1	0 – 62.7
***n*-butane / ppt**	21.9 ± 17.6	17.8	0 – 112.9
Actylene / ppt	79.0 ± 27.8	70.4	45.0 – 180.5
Isoprene / ppt	0.1 ± 0.4	0	0 – 2.6
***iso*-pentane / ppt**	3.9 ± 3.2	3.3	0 – 22.9
***n*-pentane / ppt**	4.3 ± 3.0	3.9	0 – 21.7
***n*-hexane / ppt**	1.0 ± 0.7	0.9	0 – 4.4
Ethene / ppt	43.6 ± 15.2	46.3	6.4 – 73.2
Propene / ppt	13.5 ± 3.6	13.0	6.2 - 24.1
But-1-ene / ppt	6.5 ± 1.4	6.3	3.5 – 10.6
Benzene / ppt	13.0 ± 17.0	8.3	0 – 64.4
Toluene / ppt	77.9 ± 388.8	0	0 – 2013.9
Acetaldehyde / ppt	511.8 ± 526.0	599.3	0 – 2622.6
Methanol / ppt	247.6 ± 336.2	173.3	0 – 3337.4
DMS / ppt	8.3 ± 38.3	0	0 – 291.8

Table 1: Summary of inputs to the model. Zero values indicate measurements below the limit of detection. Further details can be found in Vaughan et al. (2012) and Carpenter et al. (2010).

Deposition processes, including dry deposition and wet deposition, and diffusion are represented in the model by a first-order loss process, with the first-order rate coefficient equivalent to a lifetime of approximately 24 hours. As discussed by Stone et al. (2010), variation of the deposition lifetime between 1 hour and 5 days results in limited changes to the modelled concentrations of OH and HO_2. Loss of reactive species to aerosol surfaces is represented in the model by parameterisation of a first-order loss process to the aerosol surface (Schwarz, 1986), as discussed by Stone et al. (2014).

A range of aerosol uptake coefficients for HO_2 have been reported in the literature, with recent measurements indicating values of γ_{HO2} between 0.003 and 0.02 on aqueous aerosols (George et al., 2013) while others have reported values of $\gamma_{HO2} \sim 0.1$ (Taketani et al., 2008), and increased uptake coefficients in the presence of Cu and Fe ions (Thornton et al., 2008; Mao et al., 2013). In this work we use a value of $\gamma_{HO2} = 0.1$ in order to maintain consistency with previous modelling studies at the site (Whalley et al., 2010) and to account for potential impacts of ions of copper and iron in aerosol particles influenced by mineral dust (Carpenter et al., 2010; Muller et al., 2010; Fomba et al., 2014; Matthews et al., 2014; Lakey et al., 2015).

The aerosol surface area in the model is constrained to previous measurements of dry aerosol surface area at the observatory, corrected for differences in sampling height between the aerosol and HO_x measurements and for aerosol growth under humid conditions (Allan et al., 2009; Muller et al., 2010; Whalley et al., 2010).

Halogen species are constrained to a 'top-hat' profiles for BrO and IO (Vogt et al., 1999; Vogt et al., 1996; Read et al., 2008), as observed during the RHAMBLE campaign in 2007 (Read et al., 2008; Mahajan et al., 2010a). The observations indicate that while there is day to day variation in BrO and IO concentrations, there is little seasonal variation (Mahajan et al., 2010a). BrO and IO are thus constrained to the mean observed mixing ratios of 2.5 ppt and 1.4 ppt, respectively, for time points between 0930 and 1830 (GMT) and zero for all other times. Sensitivity to these mixing ratios is discussed in the Supplementary Material. In a similar way to NO_x (see Stone et al. (2010; 2011)), concentrations of all bromine or iodine species, including BrO and IO, are permitted to vary according to the photochemistry as the model runs forwards. At the end of each 24 hour period in the model, the calculated concentrations of BrO and IO are compared to the constrained value, and the concentrations of all bromine (Br, Br_2, BrO, HBr, HOBr, $BrONO_2$, $BrNO_2$, BrNO) and iodine (I, I_2, IO, HI, HOI, INO, INO_2, $IONO_2$, OIO, I_2O_2, I_2O_3, I_2O_4, $HOIO_2$) species are fractionally increased or decreased such that the calculated and constrained concentrations of BrO and IO are the same. The model is run forwards in time with diurnally varying photolysis rates until a diurnal steady state is reached, typically requiring between 5 and 10 days.

Global Model

We use the 3D global chemistry transport model GEOS-Chem (v10-01, www.geos-chem.org). The model has been extensively evaluated against observations (Bey et al., 2001; Evans and Jacob, 2005; Nassar et al., 2009; Mao et al., 2010; Zhang et al., 2010; Parrella et al., 2012; Hu et al., 2017). The model is driven by assimilated winds calculated by the Goddard Earth Observing System at a horizontal resolution of 4° × 5°, with 47 vertical levels from the surface to 50 hPa. Anthropogenic emissions of CO, NO_x and SO_2 are described by the EDGAR 3.2 monthly global inventory (Olivier et al., 2005). Emissions of volatile organic compounds (VOCs) are described by the RETRO monthly global inventory (van het Bolscher, 2008) for anthropogenic sources, with ethane emissions described by Xiao et al., 2008, and the MEGAN v2.1 inventory (Guenther et al., 2006; Barkley et al., 2011) for biogenic sources.

The HO_x-NO_x-VOC-O_3 chemistry scheme in the model is described in detail by Bey et al. (2001) and Mao et al. (2013), with the isoprene oxidation mechanism described by Paulot et al. (2009). Photolysis rates use the FAST-JX scheme (Bian and Prather, 2002; Mao et al., 2010), with acetone photolysis rates updated by Fischer et al. (2012). Stratospheric chemistry is based on LINOZ McLinden et al. (2000) for O_3 and a linearised mechanism for other species as described by Murray et al. (2012).

The model framework includes gas-aerosol partitioning of semi-volatile organic compounds (Liao et al., 2007; Henze et al., 2007; Henze et al., 2009; Fu et al., 2008; Heald et al., 2011; Wang et al., 2011), and heterogeneous chemistry (Jacob, 2000). Coupling between gas phase chemistry and sulfate-ammonium-nitrate aerosol is described by Park et al. (2004) and Pye et al. (2009). A description of dust aerosol in the model is given by Fairlie et al. (2007). Treatment of sea salt aerosol is described by Jaegle et al. (2011). The uptake coefficient for N_2O_5 uses the parameterisation by Evans and Jacob (2005), while that for HO_2 uses the parameterisation of Thornton et al. (2008). A full description of the organic aerosol chemistry in the model is given by Heald et al. (2011).

The model includes recent updates to the chemistry scheme to include bromine chemistry (Parella et al., 2012; Schmidt et al., 2016) and iodine chemistry (Sherwen et al., 2016a; Sherwen et al., 2016b). Sources of tropospheric bromine in the model include emissions of $CHBr_3$, CH_2Br_2 and CH_3Br, and transport of reactive bromine from the stratosphere. Debromination of sea-salt aerosol is not included in the model following the work of Schmidt et al. (2016), which showed better agreement with observations of BrO made by the GOME-2 satellite (Theys et al., 2011) and in the free troposphere and the tropical Eastern Pacific MBL (Gomez Martin et al., 2013; Volkamer et al., 2015; Wang et al., 2015). Emission rates and bromine chemistry included in the model are described in detail by Parella et al. (2012), with the bromine chemistry scheme described by 19 bimolecular reactions, 2 three-body

reactions and 2 heterogeneous reactions using rate coefficients, heterogeneous reaction coefficients and photolysis cross-sections recommended by Sander et al. (2011).

Iodine sources include emissions of CH_3I, CH_2I_2, CH_2ICl, CH_2IBr, I_2 and HOI. Emissions for CH_3I follow Bell et al. (2002), while those of other organic iodine species use parameterisations based on chlorophyll-a in the Tropics and constant oceanic and coastal fluxes in extratropical regions (Ordonez et al., 2012). Emissions of inorganic iodine species (HOI and I_2) use the results of Carpenter et al. (2013), with oceanic iodide concentrations parameterised by MacDonald et al. (2014). The iodine chemistry scheme includes 26 unimolecular and bimolecular reactions, 3 three-body reactions, 21 photolysis reactions and 7 heterogeneous reactions, using recommendations by Atkinson et al. (2007) and Sander et al. (2011) where available. Full details are given by Sherwen et al. (2016a; 2016b).

Photolysis rates of bromine and iodine compounds are calculated using the FAST-J radiative transfer model (Wild et al., 2000; Bian and Prather, 2002; Mao et al., 2010). Wet and dry deposition are determined as for the standard GEOS-Chem model (Liu et al., 2001; Wesely, 1989; Wang et al., 1998; Amos et al., 2012).

The tropospheric chemistry scheme is integrated using the SMVGEAR solver (Jacobson and Turco, 1994; Bey et al., 2001). The model, provides hourly output at the site of the Cape Verde Atmospheric Observatory. Model simulations have been performed in the absence of halogens, with bromine chemistry, with iodine chemistry and with bromine and iodine chemistry combined. Each model simulation is run for two years, with the analysis performed on the second year (2009) and the first year discarded as model spin-up to enable evolution of long-lived species.

Model Results

We now investigate the impact of halogen chemistry on tropospheric oxidation at Cape Verde within our two modelling approaches.

Constrained Box Model

Figure 1 shows the observed and modelled time series for OH and HO_2 during SOS1 (February, March 2009) and SOS2 (May, June 2009). Observed concentrations of OH and HO_2 were typically higher in SOS2 than SOS1, reaching maximum values in SOS2 of ~ 9×10^6 cm^{-3} OH and 4×10^8 cm^{-3} HO_2 (Vaughan et al., 2012). Similar concentrations were observed in May and June 2007 during the RHaMBLe campaign (Whalley et al., 2010), with a *t*-test indicating no statistically significant difference between the OH concentrations measured in May-June

2009 to those measured in May-June 2007 at the 95 % confidence level (Vaughan et al., 2012). Concentrations of HO_2 measured in May-June 2009 were significantly higher than those measured in May-June 2007 at the 95 % confidence level, but were within the 1σ day-to-day variability (Vaughan et al., 2012). Temperatures during SOS2 were typically higher than those during SOS1, with higher relative humidity during SOS2 (Vaughan et al., 2012). Air masses during SOS1 had strong contributions from Atlantic marine air and African coastal region, with polluted marine air and Saharan dust contributing ~ 20 % and 10 %, respectively, for the first half of the measurement period. Conditions during SOS2 were typically cleaner, with Atlantic marine air representing the major source, although coastal African air contributed ~ 40 % on some days. There was little influence from polluted air, dust or continental air (Vaughan et al., 2012). Analysis of the variance of OH and HO_2 during SOS indicated that ~70 % of the total variance could be explained by diurnal behaviour, with the remaining ~30 % related to changes in air mass.

Figure 1 shows the observed and modelled time series for OH and HO_2, for model simulations with and without halogen chemistry. For SOS1, the box model overpredicts the OH and HO_2 concentrations at the start of the campaign (Julian days 59 and 61), but performs better for day 63, and captures both the observed diurnal profile and the observed concentrations. For SOS2, the box model tends to agree better with the observations for both OH and HO_2. A day-by-day comparison between the models and the observations is shown in the Supplementary Material for days for which box model calculations were possible, which were limited by the availability of supporting data.

Figure 2 shows the point-by-point model performance for OH and HO_2 for all data points combined, and for SOS1 and SOS2 separately, for the full box model run including halogen chemistry. There is a tendency for overprediction of OH and HO_2 during SOS1 (slopes of modelled vs observed concentrations are (1.86 ± 0.26) for OH and (1.66 ± 0.21) for HO_2), which is dominated by the model overpredictions on days 59 and 61, with better agreement observed during SOS2 (slopes of modelled vs observed concentrations are (1.11 ± 0.15) for OH and (1.21 ± 0.12) for HO_2).

The measured and modelled average diurnal profiles of OH, HO_2 and the HO_2 to OH ratios are shown in Figure 3. At midday (1100-1300), the full model including halogen chemistry overpredicts OH by a median factor of 1.52 and HO_2 by a median factor of 1.21. A model run containing bromine chemistry but no iodine chemistry gave median midday overpredictions of 1.40 and 1.30 for OH and HO_2, respectively, while a run containing iodine but not bromine gave equivalent median overpredictions of 1.50 and 1.26, respectively. With no halogen chemistry included in the model, the modelled OH decreases, giving a median overprediction at midday by a

356 factor of 1.37, while the modelled HO_2 increases, resulting in a median overprediction by a factor of 1.37 at
357 midday.
358
359 Thus the inclusion of halogens (bromine and iodine) in the box model changes the mean noon time OH and HO_2
360 concentrations by +9.8 % and –9.9 %, respectively. This impact of halogen chemistry is consistent in sign and
361 magnitude with previous studies (Kanaya et al., 2002; Bloss et al., 2005a; Kanaya et al., 2007; Sommariva et al.,
362 2006; Sommariva et al., 2007; Whalley et al., 2010).
363
364 Figure 4 shows the mean midday total RO_x budget (given the fast processing time between HO_2 and HOBr/HOI
365 we identify the RO_x family as OH, HO_2, HOBr, HOI, RO and RO_2) for the two measurement periods during SOS
366 for model runs with and without halogens. These budgets are similar both between time periods (i.e. SOS1 vs
367 SOS2) and for box model calculations with and without halogen chemistry. Radical production dominated by
368 photolysis of ozone (~83 %), with photolysis of HCHO (~10 %), CH_3CHO (~2 %) and H_2O_2 (~2 %) playing a
369 significantly smaller role. Radical termination reactions were dominated by $HO_2 + CH_3O_2$ (~23 %), aerosol uptake
370 of HO_2 (~21 %), $HO_2 + HO_2$ (~19 %), $CH_3C(O)O_2 + HO_2$ (~8 %), and $OH + HO_2$ (~5 %). The inclusion of the
371 reaction between OH and CH_3O_2 reduces the importance of radical termination via $HO_2 + CH_3O_2$ (from ~26 %
372 of the total to ~23 % of the total), but otherwise has little impact on the total radical removal owing to the expected
373 production of $HO_2 + CH_3O$ (Assaf et al., 2017). Further details regarding the impact of the reaction between OH
374 and CH_3O_2 on the HO_2:OH ratio and CH_3O_2 budget are given in the Supplementary Material.
375
376 The budget analyses for SOS are consistent with those determined for the RHaMBLe campaign (Whalley et al.,
377 2010; Fittschen et al., 2014; Assaf et al., 2017), reflecting similarities in observed concentrations of long-lived
378 species and the method of the model constraint with observed O_3 concentrations and photolysis rates. The primary
379 source of radicals therefore remains fixed in all simulations, with the primary sinks for these species occurring
380 through radical-radical reactions. Thus, the total radical concentration and budget is little impacted by the
381 presence of halogens.
382
383 However, the partitioning of the radicals is impacted by the halogens. Without halogens the average midday
384 (1100-1300) HO_2 to OH ratio is (83.4 ± 15.4) (median = 82.7), with the halogens this changes to (68.3 ± 13.6)
385 (median = 66.9) (Table 2). This change in partitioning is mainly due to the reaction of HO_2 with BrO and IO
386 followed by the photolysis of HOBr and HOI to give OH. In this way the halogens tend to reduce the concentration
387 of HO_2 and increase the concentration of OH.
388

	HO_2:OH ratio
Observed	79.1 ± 34.1 (70.7)
Box model, no halogens	83.4 ± 15.4 (82.7)
Box model with Br chemistry	78.9 ± 15.6 (77.8)
Box model with I chemistry	71.5 ± 13.0 (70.4)
Box model with Br and I chemistry	68.3 ± 13.6 (66.9)
Global model, no halogens	80.8 ± 18.1 (78.9)
Global model with Br chemistry	81.9 ± 19.0 (79.7)
Global model with I chemistry	70.4 ± 12.5 (70.5)
Global model with Br and I chemistry	71.3 ± 13.2 (71.3)

Table 2: Mean (± 1σ) midday (1100-1300 hours) ratios of HO_2 to OH (SOS1 and SOS2 combined). Median values are given in parentheses.

In the box model without halogen chemistry, production of OH is dominated by ozone photolysis (76 %), HO_2 + NO (12 %) and HO_2 + O_3 (9 %), with OH loss controlled by OH + CO (37 %), OH + CH_4 (16 %) and OH + CH_3CHO (15 %), as shown in Figure 5. Production of HO_2 in the model excluding halogens is controlled by OH + CO (45 %), CH_3O + O_2 (19 %) and photolysis of HCHO (10 %), with loss governed by aerosol uptake (26 %), HO_2 + HO_2 (26 %), HO_2 + NO (15 %), HO_2 + CH_3O_2 (12 %) and HO_2 + O_3 (10 %). In the presence of halogens, the instantaneous budgets for OH and HO_2 are impacted by BrO and IO, as shown in Figures 5 and 6. For the model run including halogens, OH production is still dominated by ozone photolysis (68 %), but there are significant contributions from photolysis of HOI (10 %) and HOBr (3 %). Loss of HO_2 is also affected by the presence of the halogen species, with the dominant loss processes including aerosol uptake (20 %), HO_2 + HO_2 (19 %), HO_2 + IO (14 %), HO_2 + NO (12 %), HO_2 + CH_3O_2 (11 %), HO_2 + O_3 (8 %) and HO_2 + BrO (6 %). The change in the relative importance of HO_2 + NO on inclusion of halogens in the model results from both the increase in the total HO_2 sink, owing to the additional losses through HO_2 + BrO and HO_2 + IO, and the shift in NO_x partitioning owing to the reactions Br + NO → Br + NO_2 and IO + NO → I + NO_2. The reactions of BrO and IO with NO result in a change in the NO_2:NO ratio of approximately 10 %, on average, which reduces the impact of HO_2 + NO as both a sink for HO_2 and a source for OH. As shown in Figures 4-6 there is little difference in the radical budgets between SOS1 and SOS2.

This box modelling study is consistent with previous studies (Kanaya et al., 2002; Bloss et al., 2005a; Kanaya et al., 2007; Sommariva et al., 2007; Whalley et al., 2010; Mahajan et al., 2010a; Stone et al., 2012) in that it implies that halogen chemistry is likely to increase the OH concentration of the marine boundary layer (and potentially

other regions of the troposphere) as it enhances the HO_2 to OH conversion through the production of HOBr and HOI. We now look at the impact of halogen chemistry on the concentrations of OH and HO_2 at Cape Verde within the framework of a global atmospheric chemistry model.

Global Model

Figure 1 shows the time series for OH and HO_2 calculated by the global model GEOS-Chem, with the average diurnal profiles shown in Figure 3. The global model displays a significant overprediction for OH and HO_2 during SOS1, but exhibits reasonable skill at reproducing the observed concentrations during SOS2 and captures the HO_2:OH ratio for both measurement periods. The overpredictions of OH and HO_2 in the global model likely result from a combination of missing OH-sinks, particularly oxygenated volatile organic compounds (oVOCs) which are currently underestimated in the global model (Millet et al., 2015), and potential overprediction of the primary radical production rate owing to reductions in photolysis rates resulting from cloud cover that are not captured by the global model.

At midday (1100-1300), the modelled to observed ratios for OH and HO_2 for the global model excluding halogen chemistry are (1.52 ± 1.02) and (1.72 ± 0.80), respectively, with a mean modelled HO_2 to OH ratio of (80.8 ± 18.1) (compared to the observed HO_2 to OH ratio of (79.1 ± 34.1)). For the global model run including bromine chemistry, but not iodine, the mean midday modelled to observed ratios for OH and HO_2 are (1.48 ± 1.05) and (1.69 ± 0.81), respectively, with a mean midday modelled HO_2 to OH ratio of (81.9 ± 19.0). Bromine chemistry thus acts to decrease the concentrations of both OH and HO_2, in contrast to the box model results which show increased concentrations of OH and decreased concentrations of HO_2. For the model run including iodine, but not bromine, the midday modelled to observed ratios for OH and HO_2 are (1.57 ± 1.00) and (1.59 ± 0.81), respectively, with a mean midday modelled HO_2 to OH ratio of (70.4 ± 12.5). Iodine chemistry thus results in increased OH and decreased HO_2 for both the global and box model simulations at Cape Verde. Inclusion of bromine and iodine chemistry combined leads to midday modelled to observed ratios of (1.53 ± 1.01) for OH and (1.57 ± 0.82) for HO_2, and a mean midday modelled HO_2 to OH ratio of (71.3 ± 13.2). These results are shown in Table 2, alongside those for the box model.

The results from the global model at Cape Verde thus differ from those of the box model. For the box model, inclusion of bromine and iodine chemistry, whether separately or combined, leads to increased OH and decreased HO_2 through increased conversion of HO_2 to OH through the production and subsequent photolysis of HOBr and HOI. In the global model a more complex pattern emerges. In a similar way to the box model, the HO_2 concentrations in the global model are decreased on inclusion of bromine and/or iodine owing to the additional

loss reactions HO_2 + BrO and HO_2 + IO. When bromine chemistry is considered in the global model in isolation from iodine chemistry, the OH concentration decreases, despite the production and photolysis of HOBr. This decrease occurs as a result of a reduction in the O_3 concentration in the model on inclusion of bromine chemistry owing to the reaction of Br with O_3, which leads to a decrease in the rate of primary radical production from O_3 photolysis and thus lower OH concentrations. The impact of the decreased radical production rate is greater than that leading to increased OH production through HOBr photolysis, and the net OH concentration is reduced in the global model. This effect is not observed in the box model calculations as the model runs are constrained to long-lived species – including O_3. The change in O_3 concentration on the inclusion of halogen chemistry is thus not considered in the box model simulations, and the subsequent impacts of halogens consider only those changes occurring on a more rapid timescale, which lead to increases in the OH concentration.

However, the inclusion of iodine chemistry in the global model does lead to increased OH concentrations at Cape Verde. Direct emissions of HOI in the global model, in addition to chemical production through HO_2 + IO, result in increased OH production through HOI photolysis as well as the repartitioning of HO_2 and OH through HOI production in a similar manner to that for HOBr. However, the more rapid cycling of HO_2 to OH through the more rapid production and photolysis of HOI compared to HOBr, reduces the impact of iodine chemistry on the HO_2:OH ratio compared to that for bromine chemistry. Iodine chemistry thus can reduce the OH concentration similarly to bromine chemistry, through the destruction of O_3 and subsequent reduction in primary production rate, but the impact is less than that for bromine, and can be offset by the direct emissions of HOI which increases the production rate of OH through photolysis.

The impacts of iodine chemistry in the global model are thus more complex than those for bromine chemistry. When bromine and iodine chemistry are combined in the global model there is a competition between the effects of the reduction in primary production of OH, through depletion of O_3, and the production of OH from photolysis of HOBr and HOI and, for the model simulations at Cape Verde, the impacts of direct HOI emissions dominate. The OH concentration is thus marginally increased compared to simulations containing no halogens, although the HO_2 concentrations are significantly decreased.

The impacts of halogens on OH radical concentrations in the global model thus display a complexity that is somewhat obscured in the box model simulations. Overall, the inclusion of halogens in the global model leads to a slight increase in OH at Cape Verde, but, owing to the opposing effects of bromine and iodine, this result is subject to the modelled concentrations of bromine and iodine species. Observations at Cape Verde made between November 2006 and June 2007 indicate ‘top-hat’ profiles for BrO and IO, with average daytime mixing ratios of

2.5 ppt and 1.4 ppt, respectively, and little variability over the entire campaign (Read et al., 2008; Mahajan et al., 2010a). The global model simulations reported here predict average mixing ratios of ~0.5 ppt for BrO and ~1 ppt for IO during SOS, and thus underpredict BrO but perform well for IO. The underprediction of BrO at Cape Verde results from recent model updates which exclude emissions of bromine species from sea-salt debromination (Schmidt et al., 2016) in order to provide improved agreement with observations of BrO made by the GOME-2 satellite (Theys et al., 2011) and in the free troposphere and the tropical Eastern Pacific MBL (Gomez Martin et al., 2013; Volkamer et al., 2015; Wang et al., 2015). If sea-salt debromination were included, daytime mixing ratios of BrO at Cape Verde would be approximately 2 ppt, as shown by Parella et al. (2012) and Schmidt et al. (2016), and thus in closer agreement to the observations. Increased modelled concentrations of BrO at Cape Verde resulting from inclusion of sea-salt debromination would have a greater effect on OH and HO_2, leading to more significant decreases in OH and HO_2 when bromine chemistry is included without iodine chemistry, with the larger decrease in OH potentially off-setting the increase in OH observed when bromine and iodine chemistry are combined. However, the current model simulations do not consider the coupling between bromine and sulfur chemistry, which may represent a significant sink for reactive bromine species in the troposphere and balance sources from sea-salt debromination (Chen et al., 2017). These results thus demonstrate the need for further investigation and constraint of sources and emission rates of bromine species, and of the coupling between sulfur chemistry and reactive bromine species. We now discuss the global impacts of halogen chemistry.

Global impacts of halogen chemistry on OH and HO_2

On the global scale, concentrations of OH and HO_2 are reduced on inclusion of bromine and iodine chemistry, both individually and combined. The global mass weighted annual mean OH concentration decreases by 3.8 % on inclusion of bromine chemistry, but only 0.02 % on inclusion of iodine chemistry alone. When the chemistry of bromine and iodine is combined in the model, the global mass weighted annual mean OH concentration decreases by 4.5 %. For HO_2, the global mass weighted annual mean is decreased by 4.2 % by bromine, 5.6 % by iodine and 9.7 % by bromine and iodine combined. Figure 7 shows the probability distribution functions for the changes to OH and HO_2 concentrations for the monthly mean values for all grid boxes within the troposphere for the year. For the majority of grid boxes, concentrations of OH and HO_2 are reduced on inclusion of bromine chemistry, with iodine also generally reducing HO_2 concentrations but leading to a wider spread of changes to the OH concentration, and similar numbers of grid boxes showing increased and decreased concentrations. When bromine and iodine chemistry are combined in the model, HO_2 shows a more significant decrease than for either halogen individually, and OH, although exhibiting increased concentrations in a significant number of grid boxes, displays a greater tendency for decreased concentrations.

Figure 8 shows the changes to the annual modelled surface layer OH and HO_2 concentrations on inclusion of halogen chemistry, with annual surface layer mixing ratios of BrO and IO shown in Figure 9. The most significant changes to OH and HO_2 occur over marine regions, particularly over the Southern Pacific. Smaller changes are observed over land, and any increased concentrations, including those for OH over Cape Verde, can be seen to occur in coastal regions where the impacts of direct HOI emissions dominate and concentrations of IO concentrations are typically elevated.

Thus, overall, halogens act to reduce the oxidising capacity of the troposphere through reductions to O_3 and subsequent reductions in the primary production rates of OH and HO_2, despite the slight increase in OH concentration predicted by the global model at Cape Verde. Consideration of the full extent of the impacts of halogens on the global oxidising capacity is hindered by uncertainties in the concentrations and distributions of halogen species, and model representations of halogen processes, particularly those relating to sea salt debromination, ocean iodide emissions, parameterisations of iodine recycling in aerosols and photolysis of higher iodine oxides (Sherwen et al., 2016a).

Conclusions

Measurements of OH and HO_2 made by LIF-FAGE at the Cape Verde Atmospheric Observatory during the Seasonal Oxidants Study in 2009 have been simulated by a constrained box model and a three-dimensional global chemistry transport model. The observations are generally reproduced well by the box model, but are overpredicted by the global model.

The oxidising capacity of the two models, as manifested by the OH concentration, shows opposing sensitivity to halogens. The constrained box model shows an increase in OH concentrations with the inclusion of halogens, whereas the global transport model shows a decrease in OH concentrations globally, despite a marginal decrease in the OH concentration at Cape Verde. This difference between models reflects differing representation of chemical timescales by the models. The box model is constrained to concentrations of long-lived compounds, including O_3, and considers only impacts on short timescales, whereas the global model includes impacts occurring on longer timescales. Within this context, the box model includes the short timescale impact of halogens on the repartitioning of HO_2 to OH, thus increasing OH and decreasing HO_2, but does not consider the longer timescale impact of halogen-mediated ozone destruction which impacts primary radical production. This highlights a general problem with understanding the complex interactions within atmospheric chemistry and the Earth system in general. Evaluating the impact of a small part of the system on the system as a whole can be

difficult and the most significant processes may occur on timescales significantly longer than those of the perturbation.

Acknowledgements

This project was funded by the Natural Environment Research Council (NERC, NE/E011403/1), with support of the Cape Verde Atmospheric Observatory by the National Centre for Atmospheric Science (NCAS) and the SOLAS project. DS would also like to thank NERC for the award of an Independent Research Fellowship (NE/L010798/1). Computational resources were provided by the NERC BACCHUS project (NE/L01291X/1)

References

Alicke, B., Hebestriet, H., Stutz, J., Platt, U.: Iodine oxide in the marine boundary layer, Nature, 397, 572-573, 1999

Allan, J.D., Topping, D.O., Good, N., Irwin, M., Flynn, M.,Williams, P.I., Coe, H., Baker, A.R., Martino, M., Niedermeier, N., Wiedensohler, A., Lehmann, S., Muller, K., Herrmann, H.,and McFiggans, G.: Composition and properties of atmospheric particles in the eastern Atlantic and impacts on gas phase uptake rates, Atmos. Chem. Phys., 9, 9299–9314, 2009

Amos, H.M., Jacob, D.J., Holmes, C.D., Fisher, J.A., Wang, Q., Yantosca, R.M., Corbitt, E.S., Galarneau, E., Rutter, A.P., Gustin, M.S., Steffen, A., Schauer, J.J., Graydon, J.A., St. Louis, V.L., Talbot, R.W., Edgerton, E.S., Zhang, Y., and Sunderland, E.M: Gas-particle partitioning of Hg(II) and its effect on global mercury deposition, Atmos. Chem. Phys., 12, 1, 591-603, doi:10.5194/acp-12-591-2012, 2012

Assaf, E., Song, B., Tomas, A., Schoemaker, C., and Fittschen, C.: Rate constant of the reaction between CH_3O_2 and OH radicals revisited, J. Phys. Chem. A, 120, 8923-8932, 2016

Assaf, E., Sheps, L., Whalley, L., Heard, D., Tomas, A., Schoemaecker, C., and Fittschen, C.: The reaction between CH_3O_2 and OH radicals: Product yields and atmospheric implications, Environ. Sci. Technol., 51, 4, 2170-2177, doi: 10.1021/acs.est.6b06265, 2017

Atkinson, R., Baulch, D.L., Cox, R.A., Crowley, J.N., Hampson, R.F., Hynes, R.G., Jenkin, M.E., Rossi, M. J., and Troe, J.: Evaluated kinetic and photochemical data for atmospheric chemistry: Volume III – gas phase reactions of inorganic halogens, Atmos. Chem. Phys., 7, 981–1191, doi:10.5194/acp-7-981-2007, 2007

Barkley, M.P., Palmer, P.I., Ganzeveld, L., Arneth, A., Hagberg, D., Karl, T., Guenther, A., Paulot, F., Wennberg, P.O., Mao, J.Q., Kurosu, T.P., Chance, K., Muller, J.-F., De Smedt, I., van Roozendael, M., Chen, D., Wang, Y.X., and Yantosca, R.M.: Can a "state of the art" chemistry transport model simulate Amazonian tropospheric chemistry? J. Geophys. Res. Atmos., 116, D16302, 1-28, doi:10.1029/2011JD015893, 2011

Bell, N., Hsu, L., Jacob, D.J., Schultz, M.G., Blake, D.R., Butler, J.H., King, D.B., Lobert, J.M., and Maier-Reimer, E.: Methyl iodide: Atmospheric budget and use as a tracer of marine convection in global models, J. Geophys. Res. Atmos., 107, ACH 8-1–ACH 8-12, doi:10.1029/2001jd001151, 2002

Bey, I., Jacob, D.J., Yantosca, R.M., Logan, J.A., Field, B.D., Fiore, A.M., Li, Q., Liu, H.Y., Mickley, L.J., Schultz, M.G.: Global modelling of tropospheric chemistry with assimilated meteorology: Model description and evaluation, J. Geophys. Res., 106, D19, 23073-23095, 2001

Bian, H.S., and Prather, M.J.: Fast-J2: Accurate simulation of stratospheric photolysis in global chemistry models, J. Atmos. Chem., 41, 3, 281-296, 2002

Bitter, M., Ball, S., Povey, I., and Jones, R.: A broadband cavity ringdown spectrometer for in-situ measurements of atmospheric trace gases, Atmos. Chem. Phys., 5, 3491–3532, doi:10.5194/acp-8-3491-2005, 2005

Bloss, W.J., Lee, J.D., Johnson, G.P., Sommariva, R., Heard, D.E., Saiz-Lopez, A., Plane, J.M.C., McFiggans, G., Coe, H., Flynn, M., Williams, P., Rickard, A.R., Fleming, Z.: Impact of halogen monoxide chemistry upon boundary layer OH and HO_2 concentrations at a coastal site, Geophys. Res. Lett., 32, L06814, doi:10.1029/2004GL022084, 2005a

Bloss, W.J., Evans, M.J., Lee, J.D., Sommariva, R., Heard, D.E., Pilling, M.J.: The oxidative capacity of the troposphere: Coupling of field measurements of OH and a global chemistry transport model, Faraday. Discuss., 130, 425-436, 2005b

Bloss, W.J., Lee, J.D., Heard, D.E., Salmon, Bauguitte, S.J.-B., Roscoe, H.K., Jones, A.E.: Observations of OH and HO_2 radicals in coastal Antarctica, Atmos. Chem. Phys., 7, 4171-4185, 2007

Bloss, W.J., Camredon, M., Lee, J.D., Heard, D.E., Plane, J.M.C., Saiz-Lopez, A., Bauguitte, S.J.-B., Salmon, R.A., Jones, A.E.: Coupling of HO_x, NO_x and halogen chemistry in the Antarctic boundary layer, Atmos. Chem. Phys., 10, 10187-10290, 2010

Bossolasco, A., Farago, E.P., Schoemaker, C., and Fittschen, C.: Rate constant of the reaction between CH_3O_2 and OH radicals, Chem. Phys. Lett., 593, 7-13, 2014

Carpenter, L. J., Fleming, Z. L., Read, K. A., Lee, J. D., Moller, S.J., Hopkins, J., Purvis, R., Lewis, A. C., Muller, K., Heinold, B., Herrmann, H., Wadinga Fomba, K., van Pinxteren, D., Muller, C., Tegen, I., Wiedensohler, A., Muller, T., Niedermeier, N., Achterberg, E. P., Patey, M. D., Kozlova, E. A., Heimann, M., Heard, D. E., Plane, J. M. C., Mahajan, A., Oetjen, H., Ingham, T., Stone, D., Whalley, L., Evans, M., Pilling, M. J., Leigh, R. J., Monks, P. S., Karunaharan, A., Vaughan, S., Tschritter, J., Pohler, D., Frieß, U., Holla, R., Mendes, L., Lopez, H., Faria, B., Manning, A. J., and Wallace, D. W. R.: Seasonal characteristics of tropical marine boundary layer air measured at the Cape Verde Atmospheric Observatory, J. Atmos. Chem., 67, 87–140, 2010

Carpenter, L.J., MacDonald, S.M., Shaw, M.D., Kumar, R., Saunders, R.W., Parthipan, R., Wilson, J., and Plane, J.M.C.: Atmospheric iodine levels influenced by sea surface emissions of inorganic iodine, Nat. Geosci., 6, 108–111, doi:10.1038/ngeo1687, 2013

Carslaw, N., Creasey, D. J., Heard, D. E., Lewis, A .C., McQuaid, J. B., Pilling,M. J.,Monks, P. S., Bandy, B. J., and Penkett, S. A.: Modeling OH, HO_2, and RO_2 radicals in the marine boundary layer – 1. Model construction and comparison with field measurements, J. Geophys. Res., 104(D23), 30 241–30 255, 1999

Carslaw, N., Creasey, D. J., Heard, D. E., Jacobs, P. J., Lee, J. D., Lewis, A. C., McQuaid, J. B., Pilling, M. J., Bauguitte, S., Penkett, S. A., Monks, P. S., Salisbury, G.: Eastern Atlantic Spring Experiment 1997 (EASE97) – 2. Comparisons of model concentrations of OH, HO_2, and RO_2 with measurements, J. Geophys. Res.-Atmos., 107(D14), 4190, 2002

Chen, Q., Schmidt, J.A., Shah, V., Jaegle, L., Sherwen, T., and Alexander, B.: Sulfate production by reactive bromine: Implications for the global sulfur and reactive bromine budgets, Geophys. Res. Lett., 44, 7069-7078, doi:10.1002/2017GL073812, 2017

Commane, R., Seitz, K., Bale, C.S.E., Bloss, W.J., Buxmann, J., Ingham, T., Platt, U., Pohler, D., Heard, D.E.: Iodine monoxide at a clean marine coastal site: observations of high frequency variations and inhomogeneous distributions, Atmos. Chem. Phys., 11, 6721-6733, 2011

Dix, B., Baidar, S., Bresch, J.F., Hall, S.R., Schmidt, S., Wang, S., Volkamer, R.: Detection of iodine monoxide in the tropical free troposphere, Proc. Nat. Acad. Sci., 110, 6, 2035-2040

Edwards, P., Evans, M.J., Commane, R., Ingham, T., Stone, D., Mahajan, A.S., Oetjen, H., Dorsey, J.R., Hopkins, J.R., Lee, J.D., Moller, S.J., Leigh, R., Plane, J.M.C., Carpenter, L.J., Heard, D.E.: Hydrogen oxide photochemistry in the northern Canadian spring time boundary layer, J. Geophys. Res., 116, D22306. Doi:10.1029/2011JD016390, 2011

Ehhalt, D.H., Rohrer, F.: The tropospheric cycle of H_2: a critical review, Tellus, 61B, 500-535, 2009

Emmerson, K.M., Evans, M.J.: Comparison of tropospheric gas-phase chemistry schemes for use within global models, Atmos. Chem. Phys., 9, 1831-1845, 2009

Evans, M. J., Jacob, D. J.: Impact of new laboratory studies of N2O5 hydrolysis on global model budgets of tropospheric nitrogen oxides, ozone, and OH, Geophys. Res. Lett., 32, 1–4, 2005

Fairlie, T.D., Jacob, D.J., and Park, R.J.: The impact of transpacific transport of mineral dust in the United States, Atmos. Environ., 41, 6, 1251-1266, doi:10.1016/j.atmosenv.2006.09.048, 2007

Fischer, E.V., Jacob, D.J., Millet, D.B., Yantosca, R.M.,and Mao, J.: The role of the ocean in the global atmospheric budget of acetone, Geophys. Res. Lett., 39, L01807, doi:10.1029/2011gl050086, 2012

Fittschen, C., Whalley, L.K., and Heard, D.E.: The reaction of CH_3O_2 radicals with OH radicals: A neglected sink for CH_3O_2 in the remote atmosphere, Environ. Sci. Technol., 118, 7700-7701, 2014

Fomba, K.W., Muller, K., van Pinxteren, D., Poulain, L., van Pinxteren, M., and Herrmann, H., Long-term chemical characterization of tropical and marine aerosols at the Cape Verde Atmospheric Observatory (CVAO) from 2007 to 2011, Atmos. Chem. Phys., 14, 17, 8883-8904, doi:10.5194/acp-14-8883-2014, 2014

Fu, T.-M., Jacob, D.J., Wittrock, F., Burrows, J.P., Vrekoussis, M., and Henze, D.K.: Global budgets of atmospheric glyoxal and methylglyoxal, and implications for formation of secondary organic aerosols, J. Geophys. Res., 113, D15303, doi:10.1029/2007jd009505, 2008

Fuchs, H., Bohn, B., Hofzumahaus, A., Holland, F., Lu, K. D., Nehr, S., Rohrer, F., Wahner, A.: Detection of HO_2 by laser induced fluorescence: calibration and interferences from RO_2 radicals, Atmos. Meas. Tech., 4, 1209–1225, 2011

George, I.J., Matthews, P.S.J., Whalley, L.K., Brooks, B., Goddard, A., Baeza-Romero, M.T., Heard, D.E.: Measurements of uptake coefficients for heterogeneous loss of HO_2 onto submicron inorganic salt aerosols, Phys. Chem. Chem. Phys., 15, 12829-12845, 2013

Gomez Martin, J.C., Mahajan, A.S., Hay, T.D., Prados-Roman, C., Ordonez, C., MacDonald, S.M., Plane, J.M.C., Sorribas, M., Gil, M., Francisco Paredes Mora, J., Agama Reyes, M.V., Oram, D.E., Leedham, E., Saiz-Lopez, A.: Iodine chemistry in the eastern Pacific marine boundary layer, J. Geophys. Res. Atmos., 118, 887-904, 2013

Guenther, A., Karl, T., Harley, P., Wiedinmyer, C., Palmer, P.I., and Geron, C.: Estimates of global terrestrial isoprene emissions using MEGAN (Model of Emissions of Gases and Aerosols from Nature), Atmos. Chem. Phys., 6, 3181-3210, 2006

Heald, C.L., Coe, H., Jimenez, J.L., Weber, R.J., Bahreini, R., Middlebrook, A.M., Russell, L.M., Jolleys, M., Fu, T.M., Allan, J.D., Bower, K.N., Capes, G., Crosier, J., Morgan, W.T., Robinson, N.H., Williams, P.I., Cubison, M.J., De Carlo, P.F., and Dunlea, E.J.: Exploring the vertical profile of atmospheric organic aerosol: comparing 17 aircraft field campaigns with a global model, Atmos. Chem. Phys., 11, 24, 12673-12696, doi:10.5194/acp-11-12673-2011, 2011

Heard, D. E., Read, K. A., Methven, J., Al-Haider, S., Bloss, W. J., Johnson, G. P., Pilling, M. J., Seakins, P. W., Smith, S. C., Sommariva, R., Stanton, J. C., Still, T. J., Ingham, T., Brooks, B., De Leeuw, G., Jackson, A. V., McQuaid, J. B., Morgan, R., Smith, M. H., Carpenter, L. J., Carslaw, N., Hamilton, J., Hopkins, J. R., Lee, J. D., Lewis, A. C., Purvis, R. M., Wevill, D. J., Brough, N., Green, T., Mills, G., Penkett, S. A., Plane, J. M. C., Saiz-Lopez, A., Worton, D., Monks, P. S., Fleming, Z., Rickard, A. R., Alfarra, M. R., Allan, J. D., Bower, K., Coe, H., Cubison, M., Flynn, M., McFiggans, G., Gallagher, M., Norton, E. G., O'Dowd, C. D., Shillito, J., Topping, D., Vaughan, G., Williams, P., Bitter, M., Ball, S. M., Jones, R. L., Povey, I. M., O'Doherty, S., Simmonds, P. G., Allen, A., Kinnersley, R. P., Beddows, D. C. S., Dall'Osto, M., Harrison, R. M., Donovan, R. J., Heal, M. R., Jennings, S. G., Noone, C., Spain, G.: The North Atlantic Marine Boundary Layer Experiment (NAMBLEX).

Overview of the campaign held at Mace Head, Ireland, in summer 2002, Atmos. Chem. Phys., 6, 2241–2272, doi:10.5194/acp-6-2241-2006, 2006

Henze, D.K., Hakami, A., and Seinfeld, J.H.: Development of the adjoint of GEOS-Chem, Atmos. Chem. Phys., 7, 9, 2413-2433, 2007

Henze, D.K., Seinfeld, J.H., and Shindell, D.T.: Inverse modeling and mapping US air quality influences of inorganic PM2.5 precursor emissions using the adjoint of GEOS-Chem, Atmos. Chem. Phys., 9, 16, 5877-5903, 2009

Hoffmann, T., O'Dowd, C.D., and Seinfeld, J.H.: Iodine oxide homogeneous nucleation: An explanation for coastal new particle production, Geophys. Res. Lett., 28, 10, 1949-1952, doi:10.1029/2000GL012399, 2001

Holmes, C.D., Jacob, D.J., and Yang, X.: Global lifetime of elemental mercury against oxidation by atomic bromine in the free troposphere, Geophys. Res. Lett., 33, L20808, doi:10.1029/2006gl027176, 2006

Holmes, C.D., Jacob, D.J., Corbitt, E.S., Mao, J., Yang, X., Talbot, R., and Slemr, F.: Global atmospheric model for mercury including oxidation by bromine atoms, Atmos. Chem. Phys., 10, 12037–12057, doi:10.5194/acp-10-12037-2010, 2010

Hu, L., Jacob, D.J., Liu, X., Zhang, Y., Zhang, L., Kim, P.S., Sulprizio, M.P., and Yantosca, R.M.: Global budget of tropospheric ozone: Evaluating recent model advances with satellite (OMI), aircraft (IAGOS), and ozonesonde observations, Atmos. Environ., doi:10.1016/j.atmosenv.2017.08.036, 2017

Jacob, D.J.: Heterogeneous chemistry and tropospheric ozone, Atmos. Environ., 34, 2131–2159, doi:10.1016/S1352- 2310(99)00462-8, 2000

Jacobson, M.Z. and Turco, R.P.: SMVGEAR: A sparse-matrix, vectorized gear code for atmospheric models, Atmos. Environ., 28, 273–284, 1994

Jaeglé, L., Quinn, P.K., Bates, T.S., Alexander, B., and Lin, J.-T.: Global distribution of sea salt aerosols: new constraints from in situ and remote sensing observations, Atmos. Chem. Phys., 11, 3137–3157, doi:10.5194/acp-11-3137-2011, 2011

Jenkin, M.E., Saunders, S.M., Wagner, V., Pilling, M.J., Protocol for the development of the Master Chemical Mechanism, MCM v3 (Part B): tropospheric degradation of aromatic volatile organic compounds, Atmos. Chem. Phys., 3, 181–193, 2003

Kanaya, Y., Matsumoto, J., Kato, S., and Akimoto, H.: Behavior of OH and HO_2 radicals during the Observations at a Remote Island of Okinawa (ORION99) field campaign. 2. Comparison between observations and calculations, J. Geophys. Res.-Atmos., 106, 24209–24223, 2001

Kanaya, Y., Yokouchi, Y., Matsumoto, J., Nakamura, K., Kato, S., Tanimoto, H., Furutani, H., Toyota, K., and Akimoto, H.: Implications of iodine chemistry for daytime HO_2 levels at Rishiri Island, Geophys. Res. Lett., 29, 1212, doi:10.1029/2001GL014061, 2002

Kanaya, Y., Cao, R., Kato, S., Miyakawa, Y., Kajii, Y., Tanimoto, H., Yokouchi, Y., Mochida, M., Kawamura, K., Akimoto, H.: Chemistry of OH and HO_2 radicals observed at Rishiri Island, Japan, in September 2003: Missing daytime sink of HO_2 and positive nighttime correlations with monoterpenes, J. Geophys. Res.-Atmos., 112, D11308, doi:10.1029/2006JD007987, 2007

Lakey, P.S.J., George, I.J., Whalley, L.K., Baeza-Romero, M.T., and Heard, D.E.: Measurements of HO_2 update coefficients onto single component organic aerosols, Environ. Sci. Technol., 49, 8, 4878-4885, doi:10.1021/acs.est.5b00948, 2015

Lee, J.D., Moller, S.J., Read, K.A., Lewis, A.C., Mendes, L., Carpenter, L.J.: Year-round measurements of nitrogen oxides and ozone in the tropical North Atlantic marine boundary layer, J. Geophys. Res., 114, D21302, doi:10.1029/2009JD011878, 2009

Lee, J. D., McFiggans, G., Allan, J. D., Baker, A. R., Ball, S. M., Benton, A. K., Carpenter, L. J., Commane, R., Finley, B. D., Evans, M., Fuentes, E., Furneaux, K., Goddard, A., Good, N., Hamilton, J. F., Heard, D. E., Herrmann, H., Hollingsworth, A., Hopkins, J. R., Ingham, T., Irwin, M., Jones, C. E., Jones, R. L., Keene, W. C., Lawler, M. J., Lehmann, S., Lewis, A. C., Long, M. S., Mahajan, A., Methven, J., Moller, S. J., Mller, K., Muller, T., Niedermeier, N., O'Doherty, S., Oetjen, H., Plane, J. M. C., Pszenny, A. A. P., Read, K. A., Saiz-Lopez, A., Saltzman, E. S., Sander, R., von Glasow, R., Whalley, L., Wiedensohler, A., Young, D.: Reactive Halogens in the Marine Boundary Layer (RHaMBLe): the tropical North Atlantic experiments, Atmos. Chem. Phys., 10, 1031–1055, 2010

Le Breton, M., Bannan, T.J., Shallcross, D.E., Khan, A.M., Evans, M.J., Lee, J., Lidster, R., Andrews, S., Carpenter, L.J., Schmidt, J., Jacob, D., Harris, N.R.P., Bauguitte, S., Gallagher, M., Bacak, A., Leather, K.E., and Percival, C.J.: Enhanced ozone loss by active inorganic bromine chemistry in the tropical troposphere, Atmos. Environ., 155, 21-28, doi:10.1016/j.atmosenv.2017.02.003, 2017

Leser, H., Honninger, G., Platt, U.: MAX-DOAS measurements of BrO and NO_2 in the marine boundary layer, Geophys. Res. Lett., 30, doi:10.1029/2002GL015 811, 2003

Liao, H., Henze, D.K., Seinfeld, J.H., Wu, S.L., and Mickley, L.J.: Biogenic secondary organic aerosol over the United States: Comparison of climatological simulations with observations, J. Geophys. Res. Atmos., 112, D6, D06201, 1-19, doi:10.1029/2006JD007813, 2007

Liu, H., Jacob, D.J., Bey, I., and Yantosca, R.M.: Constraints from ^{210}Pb and ^{7}Be on wet deposition and transport in a global three-dimensional chemical tracer model driven by assimilated meteorological fields, J. Geophys. Res., 106, 12109–12128, doi:10.1029/2000jd900839, 2001

MacDonald, S.M., Gómez Martín, J.C., Chance, R., Warriner, S., Saiz-Lopez, A., Carpenter, L.J., and Plane, J.M.C.: A laboratory characterisation of inorganic iodine emissions from the sea surface: dependence on oceanic variables and parameterisation for global modelling, Atmos. Chem. Phys., 14, 5841–5852, doi:10.5194/acp-14-5841-2014, 2014

Mahajan, A.S., Plane, J.M.C., Oetjen, H., Mendes, L., Saunders, R.W., Saiz-Lopez, A., Jones, C.E., Carpenter, L.J., McFiggans, G.B.: Measurement and modelling of tropospheric reactive halogen species over the tropical Atlantic Ocean, Atmos. Chem. Phys., 10, 4611-4624, 2010a

Mahajan, A.S., Whalley, L.K., Kozlova, E., Oetjen, H., Mendez, L., Furneaux, K.L., Goddard, A., Heard, D.E., Plane, J.M.C., Saiz-Lopez, A.: DOAS observations of formaldehyde and its impact on the HO_x balance in the tropical Atlantic marine boundary layer, J. Atmos. Chem., 66, 167-178, 2010b

Mahajan, A. S., Sorribas, M., Gomez Martn, J. C., MacDonald, S. M., Gil, M., Plane, J. M. C., Saiz-Lopez, A.: Concurrent observations of atomic iodine, molecular iodine and ultrafine particles in a coastal environment, Atmos. Chem. Phys., 11, 2545–2555, doi:10.5194/acp-11-2545-2011, 2011

Mao, J., Jacob, D.J., Evans, M.J., Olson, J.R., Ren, X., Brune, W.H., Clair, J.M. St., Crounse, J.D., Spencer, K.M., Beaver, M.R., Wennberg, P.O., Cubison, M.J., Jimenez, J.L., Fried, A., Weibring, P., Walega, J.G., Hall, S.R., Weinheimer, A.J., Cohen, R.C., Chen, G., Crawford, J.H., McNaughton, C., Clarke, A.D., Jaegle, L., Fisher, J.A., Yantosca, R.M., Le Sager, P., and Carouge, C.: Chemistry of hydrogen oxide radicals (HO_x) in the Arctic troposphere in spring, Atmos. Chem. Phys., 10, 5823–5838, doi:10.5194/acp-10-5823-2010, 2010

Mao, J., Fan, S., Jacob, D.J., Travis, K.R.: Radical loss in the atmosphere from Cu-Fe redox coupling in aerosols, Atmos. Chem. Phys., 13, 509-519, 2013

Matthews, P.S.J., Baeza-Romero, M.T., Whalley, L.K., and Heard, D.E.: Uptake of HO_2 radicals onto Arizona test dust particles using an aerosol flow tube, Atmos. Chem. Phys., 14, 7397-7408, doi:10.5194/acp-14-7397-2014, 2014

McFiggans, G., Coe, H., Burgess, R., Allan, J., Cubison, M., Alfarra, M. R., Saunders, R., Saiz-Lopez, A., Plane, J. M. C., Wevill, D., Carpenter, L., Rickard, A. R., Monks, P. S.: Direct evidence for coastal iodine particles from *Laminaria* macroalgae – linkage to emissions of molecular iodine, Atmos. Chem. Phys., 4, 701–713, doi:10.5194/acp-4-701-2004, 2004

McFiggans, G., Bale, C. S. E., Ball, S. M., Beames, J. M., Bloss, W.J., Carpenter, L. J., Dorsey, J., Dunk, R., Flynn, M. J., Furneaux, K. L., Gallagher, M. W., Heard, D. E., Hollingsworth, A. M., Hornsby, K., Ingham, T., Jones, C. E., Jones, R. L., Kramer, L. J., Langridge, J. M., Leblanc, C., LeCrane, J.-P., Lee, J. D., Leigh, R. J., Longley, I., Mahajan, A. S., Monks, P. S., Oetjen, H., Orr-Ewing, A. J., Plane, J. M. C., Potin, P., Shillings, A. J. L., Thomas, F., von Glasow, R., Wada, R., Whalley, L. K., Whitehead, J. D.: Iodine-mediated coastal particle formation: an overview of the Reactive Halogens in the Marine Boundary Layer (RHaMBLe) Roscoff coastal study, Atmos. Chem. Phys., 10, 2975–2999, doi:10.5194/acp-10-2975-2010, 2010

McLinden, C.A., Olsen, S.C., Hannegan, B., Wild, O., Prather, M.J., and Sundet, J.: Stratospheric ozone in 3-D models: A simple chemistry and the cross-tropopause flux, J. Geophys. Res., 105, 14653–14665, 2000

Millet, D.B., Bassandorj, M., Farmer, D.K., Thornton, J.A., Baumann, K., Brophy, P., Chaliyakunnel, S., de Gouw, J.A., Graus, M., Hu, L., Koss, A., Lee, B.H., Lopez-Hilfiker, F.D., Neuman, J.A., Paulot, F., Peischl, J., Pollack, I.B., Ryerson, T.B., Warneke, C., Williams, B.J., and Xu, J.: A large and ubiquitous source of atmospheric formic acid, Atmos. Chem. Phys., 15, 6283-6304, doi:10.5194/acp-15-6283-2015, 2015

Muller, K., Lehmann, S., van Pinxteren, D., Gnauk, T., Niedermeier, N., Wiedensohler, A., Herrmann, H.: Particle characterization at the Cape Verde atmospheric observatory during the 2007 RHaMBLe intensive, Atmos. Chem. Phys., 10, 2709-2721, 2010

Murray, L.T., Jacob, D.J., Logan, J.A., Hudman, R.C., and Koshak, W.J.: Optimized regional and interannual variability of lightning in a global chemical transport model constrained by LIS/OTD satellite data, J. Geophys. Res. Atmos., 117, D20307, doi:10.1029/2012JD017934, 2012

Nassar, R., Logan, J. A., Megretskaia, I. A., Murray, L. T., Zhang, L., and Jones, D. B. A.: Analysis of tropical tropospheric ozone, carbon monoxide, and water vapour during the 2006 El Nino using TES observations and the GEOS-Chem model, J. Geophys. Res., 114, D17304, doi:10.1029/2009JD011760, 2009

NOAA CMDL flask analysis, ftp://ftp.cmdl.noaa.gov/ccg/ch4/, GLOBALVIEW-CH4, 2010-2011: Cooperative Atmospheric Data Integration Project – Methane. CD-ROM, NOAA ESRL, Boulder, Colorado, also available on Internet via anonymous FTP to ftp://ftp.cmdl.noaa.gov/ccg/ch4/, path: ccg/CH4/GLOBALVIEW, 2009, access: 17 Feb 2010

Novelli, P.C., Lang, P.M., Masarie, K.A., Hurst, D.F., Myers, R., Elkins, J.W.: Molecular hydrogen in the troposphere: Global distribution and budget, J. Geophys. Res., 104, D23, 30,427-30,444, 1999

O'Dowd, C.D. and Hoffmann, T.: Coastal new particle formation: a review of the current state-of-the-art, Environ. Chem., 2, 245, doi:10.1071/EN05077, 2005

Olivier, J.G.J., and Peters, J.A.H.W.: CO_2 from non-energy use of fuels: A global, regional and national perspective based on the IPCC Tier 1 approach, Res. Conserv., Recycl., 45, 3, 210-225, doi:10.1016/j.resconrec.2005.05.008, 2005

Ordonez, C., Lamarque, J.-F., Tilmes, S., Kinnison, D.E., Atlas, E.L., Blake, D.R., Sousa Santos, G., Brasseur, G., Saiz-Lopez, A.: Bromine and iodine chemistry in a global chemistry-climate model: description and evaluation of very short-lived oceanic sources, Atmos. Chem. Phys., 12, 1423-1447, 2012

Park, R.J., Jacob, D.J., Field, B.D., Yantosca, R.M., and Chin, M.: Natural and transboundary pollution influences on sulfate-nitrate-ammonium aerosols in the United States: Implications for policy, J. Geophys. Res. Atmos., 109, D15204, doi:10.1029/2003JD004473, 2004

Parrella, J.P., Jacob, D.J., Liang, Q., Zhang, Y., Mickley, L.J., Miller, B., Evans, M.J., Yang, X., Pyle, J.A., Theys, N., Van Roozendael, M.: Tropospheric bromine chemistry: implications for present and pre-industrial ozone and mercury, Atmos. Chem. Phys., 12, 6723-6740, 2012

Paulot, F., Crounse, J.D., Kjaergaard, H.G., K¨urten, A., St. Clair, J.M., Seinfeld, J.H., and Wennberg, P.O.: Unexpected Epoxide Formation in the Gas-Phase Photooxidation of Isoprene, Science, 325, 730–733, 2009

Peters, C., Pechtl, S., Stutz, J., Hebestreit, K., Honninger, G., Heumann, K. G., Schwarz, A., Winterlik, J., and Platt, U.: Reactive and organic halogen species in three different European coastal environments, Atmos. Chem. Phys., 5, 3357–3375, doi:10.5194/acp-5-3357-2005, 2005

Pye, H.O.T., Liao, H., Wu, S., Mickley, L.J., Jacob, D.J., Henze, D.K., and Seinfeld, J.H.: Effect of changes in climate and emissions on future sulfate-nitrate-ammonium aerosol levels in the United States, J. Geophys. Res. Atmos., 114, D01205, doi:10.1029/2008JD010701, 2009

Read, K. A., Mahajan, A. S., Carpenter, L. J., Evans, M. J., Faria, B. V. E., Heard, D. E., Hopkins, J. R., Lee, J. D., Moller, S. J., Lewis, A. C., Mendes, L., McQuaid, J. B., Oetjen, H., Saiz-Lopez, A., Pilling, M. J., Plane, J. M. C.: Extensive halogen mediated ozone destruction over the tropical Atlantic Ocean, Nature, 453, 7199, 1232–1235, 2008

Saiz-Lopez, A. and Plane, J. M. C.: Novel iodine chemistry in the marine boundary layer, Geophys. Res. Lett., 31, L04112, doi:10.1029/2003GL019215, 2004

Saiz-Lopez, A., Plane, J. M. C., Shillito, J. A.: Bromine oxide in the mid-latitude marine boundary layer, Geophys. Res. Lett., 31, L03111, doi:10.1029/2003GL018956, 2004

Saiz-Lopez, A., Shillto, J.A., Coe, H., Plane, J.M.C.: Measurements and modelling of I_2, IO, OIO, BrO and NO_3 in the mid-latitude marine boundary layer, Atmos. Chem. Phys., 6, 1513-1528, 2006

Saiz-Lopez, A., Lamarque, J.-F., Kinnison, D.E., Tilmes, S., Ordonez, C., Orlando, J.J., Conley, A.J., Plane, J.M.C., Mahajan, A.S., Sousa Santos, G., Atlas, E.L., Blake, D.R., Sander, S.P., Schauffler, S., Thompson, A.M., Brasseur, G.: Estimating the climate significance of halogen-driven ozone loss in the tropical marine troposphere, Atmos. Chem. Phys., 12, 3939-3949, 2012

Saiz-Lopez, A., von Glasow, R.: Reactive halogen chemistry in the troposphere, Chem. Soc. Rev., 41, 6448-6472, 2012

Sander, R., Keene, W. C., Pszenny, A. A. P., Arimoto, R., Ayers, G. P., Baboukas, E., Cainey, J. M., Crutzen, P. J., Duce, R. A., Honninger, G., Huebert, B. J., Maenhaut, W., Mihalopoulos, N., Turekian, V. C., Van Dingenen, R.: Inorganic bromine in the marine boundary layer: a critical review, Atmos. Chem. Phys., 3, 1301–1336, doi:10.5194/acp-3-1301-2003, 2003

Sander, S.P., Friedl, R.R., Abbatt, J.P.D., Barker, J.R., Burkholder, J.B., Golden, D.M., Kolb, C.E., Kurylo, M.J., Moortgat, G.K., Wine, P., Huie, R.E., and Orkin, V.L.: Chemical kinetics and photochemical data for use in atmospheric studies, Evaluation Number 17, Tech. rep., NASA Jet Propulsion Laboratory, Pasadena, 2011

Sandu, A., Sander, R.: Technical note: Simulating chemical systems in Fortran90 and Matlab with the Kinetic PreProcessor KPP-2.1, Atmos. Chem. Phys., 6, 187-195, 2006

Saunders, S.M., Jenkin, M.E., Derwent, R.G., Pilling, M.J.: Protocol for the development of the Master Chemical Mechanism, MCM v3 (Part A): tropospheric degradation of non-aromatic volatile organic compounds, Atmos. Chem. Phys., 3, 161-180, 2003

Schmidt, J.A., Jacob, D.J., Horowitz, H.M., Hu, L., Sherwen, T., Evans, M.J., Liang, Q., Suleiman, R.M., Oram, D.E., Breton, M.L., Percival, C.J., Wang, S., Dix, B., and Volkamer, R.: Modeling the observed tropospheric BrO background: Importance of multiphase chemistry and implications for ozone, OH, and mercury, J. Geophys. Res. Atmos., 121, 19, 11819-11835, doi:10.1002/2015JD024229, 2016

Schwarz, S. E.: Mass-transport considerations pertinent to aqueous phase reactions of gases in liquid-water clouds, Chemistry of Multiphase Atmospheric Systems, NATO ASI Series, G6, Jaeschke ed., Springer-Verlag, Berlin, 415–471, 1986

Sherwen, T., Evans, M.J., Carpenter, L.J., Andrews, S.J., Lidster, R.T., Dix, B., Koenig, T.K., Sinreich, R., Ortega, I., Volkamer, R., Saiz-Lopez, A., Prados-Roman, C., Mahajan, A. S., and Ordóñez, C.: Iodine's impact on tropospheric oxidants: a global model study in GEOS-Chem, Atmos. Chem. Phys., 16, 1161– 1186, doi:10.5194/acp-16-1161-2016, 2016a

Sherwen, T., Schmidt, J.A., Evans, M.J., Carpenter, L.J., Groβmann, K., Eastham, S.D., Jacob, D.J., Dix, B., Koenig, T.K., Sinreich, R., Ortega, I., Volkamer, R., Saiz-Lopez, A., Prados-Roman, C., Mahajan, A.S., and Ordóñez, C.: Global impacts of tropospheric halogens (Cl, Br, I) on oxidants and composition in GEOS-Chem, Atmos. Chem. Phys., 16, 12239-12271, doi:10.5194/acp-16-12239-2016, 2016b

Sherwen, T.M., Evans, M.J., Spracklen, D.V., Carpenter, L.J., Chance, R., Baker, A.R., Schmidt, J.A., and Breider, T.J.: Global modeling of tropospheric iodine aerosol, Geophys, Res. Lett., 43, 18, 19912-10019, doi:1002/2016GL070062, 2016c

Sherwen, T., Evans, M.J., Carpenter, L.J., Schmidt, J.A., and Mickley, L.J.: Halogen chemistry reduces tropospheric O_3 radiative forcing, Atmos. Chem. Phys., 17, 1557-1569, doi:10.5194/acp-17-1557-2017, 2017

Simpson, W.R., Brown, S.S., Saiz-Lopez, A., Thornton, J.A., and von Glasow, R.: Tropospheric Halogen Chemistry: Sources, Cycling, and Impacts, Chem. Rev., 115, 4035–4062, doi:10.1021/cr5006638, 2015

Smith, S. C., Lee, J. D., Bloss, W. J., Johnson, G. P., Ingham, T., Heard, D. E.: Concentrations of OH and HO_2 radicals during NAMBLEX: measurements and steady state analysis, Atmos. Chem. Phys., 6, 1435–1453, 2006

Sommariva, R., Bloss, W.J., Brough, N., Carslaw, N., Flynn, M., Haggerstone, A.-L., Heard, D.E., Hopkins, J.R., Lee, J.D., Lewis, A.C., McFiggans, G., Monks, P.S., Penkett, S.A., Pilling, M.J., Plane, J.M.C., Read, K.A., Saiz-Lopez, A., Rickard, A.R., Williams, P.I.: OH and HO_2 chemistry during NAMBLEX: role of oxygenates, halogen oxides and heterogeneous uptake, Atmos. Chem. Phys., 6, 1135-1153, 2006

Sommariva, R., Pilling, M.J., Bloss, W.J., Heard, D.E., Lee, J.D., Fleming, Z.L., Monks, P.S., Plane, J.M.C., Saiz-Lopez, A., Ball, S.M., Bitter, M., Jones, R.L., Brough, N., Penkett, S.A., Hopkins, J.R., Lewis, A.C., Read, K.A.: Night-time radical chemistry during the NAMBLEX campaign, Atmos. Chem. Phys., 7, 587-598, 2007

Stone, D., Evans, M.J., Commane, R., Ingham, T., Floquet, C.F.A., McQuaid, J.B., Brookes, D.M., Monks, P.S., Purvis, R., Hamilton, J.F., Hopkins, J., Lee, J., Lewis, A.C., Stewart, D., Murphy, J.G., Mills, G., Oram, D., Reeves, C.E., Heard, D.E. : HO_x observations over West Africa during AMMA: Impact of isoprene and NO_x, Atmos. Chem. Phys., 10, 9415-9429, 2010

Stone, D., Evans, M.J., Edwards, P.M., Commane, R., Ingham, T., Rickard, A.R., Brookes, D.M., Hopkins, J., Leigh, R.J., Lewis, A.C., Monks, A.C., Monks, P.S., Oram, D., Reeves, C.E., Stewart, D., Heard, D.E.: Isoprene oxidation mechanisms: measurements and modelling of OH and HO_2 over a South-East Asian tropical rainforest during the OP3 field campaign, Atmos. Chem. Phys., 11, 6749-6771, 2011

Stone, D., Whalley, L.K., Heard, D.E.: Tropospheric OH and HO_2 radicals: Field measurements and model comparisons, Chem. Soc. Rev., 41, 6348-6404, 2012

Stone, D., Evans, M.J., Walker, H., Ingham, T., Vaughan, S., Ouyang, B., Kennedy, O.J., McLeod, M.W., Jones, R.L., Hopkins, J., Punjabi, S., Lidster, R., Hamilton, J.F., Lee, J.D., Lewis, A.C., Carpenter, L.J., Forster, G., Oram, D..E., Reeves, C.E., Bauguitte, S., Morgan, W., Coe, H., Aruffo, E., Dari-Salisburgo, C., Giammaria, F., Di Carlo, P., and Heard, D.E.: Radical Chemistry at Night: Comparisons between observed and modeled HO_x, NO_3 and N_2O_5 during the RONOCO project, Atmos. Chem. Phys., 14, 1299-1321, 2014, doi:10.5194/acp-14-1299-2014

Taketani, F., Kanaya, Y., Akimoto, H.: Kinetics of heterogeneous reactions of HO_2 radical at ambient concentration levels with $(NH_4)_2SO_4$ and NaCl aerosol particles, J. Phys. Chem. A., 112, 11, 2370-2377, 2008

Theys, N., Van Roozendael, M., Hendrick, F., Yang, X., De Smedt, I., Richter, A., Begoin, M., Errera, Q., Johnston, P.V., Kreher, K., and De Mazière, M.: Global observations of tropospheric BrO columns using GOME-2 satellite data, Atmos. Chem. Phys., 11, 1791–1811, doi:10.5194/acp-11-1791-2011, 2011

Thornton, J.A., Jaegle, L., and McNeill, V.F.: Assessing known pathways for HO_2 loss in aqueous atmospheric aerosols: Regional and global impacts on tropospheric oxidants, J. Geophys. Res. Atmos., 113, D5, D05303, 1-16, doi:10.1029/2007JD009236, 2008

van het Bolscher, M., REanalysis of the TROpospheric chemical composition over the past 40 years: A long-term global modeling study of tropospheric chemistry funded under the 5th EU framework programme, *Rep. EU-Contract No. EVK2-CT-2002-00170*, 1-77, MPI for Meteorology, Hamburg, Germany

Vaughan, S., Ingham, T., Whalley, L.K., Stone, D., Evans, M.J., Read, K.A., Lee, J.D., Moller, S.J., Carpenter, L.J., Lewis, A.C., Fleming, Z.L., Heard, D.E.: Seasonal observations of OH and HO_2 in the remote tropical marine boundary later, Atmos. Chem. Phys., 12, 2149-2172, 2012

Vogt, R., Crutzen, P., and Sander, R.: A mechanism for halogen release from sea-salt aerosol in the remote marine boundary layer, Nature, 383, 327–330, 1996

Vogt, R., Sander, R., von Glasow, R., and Crutzen, P. J.: Iodine chemistry and its role in halogen activation and ozone loss in the marine boundary layer: A model study, J. Atmos. Chem., 32, 375–395, 1999

Volkamer, R., Baidar, S., Campos, T.L., Coburn, S., DiGangi, J.P., Dix, B., Eloranta, E.W., Koenig, T.K., Morley, B., Ortega, I., Pierce, B.R., Reeves, M., Sinreich, R., Wang, S., Zondlo, M.A., and Romashkin, P.A.: Aircraft measurements of BrO, IO, glyoxal, NO_2, H_2O, O_2-O_2 and aerosol extinction profiles in the tropics: comparison with aircraft-/ship-based in situ and lidar measurements, Atmos. Meas. Tech., 8, 2121–2148, doi:10.5194/amt-8-2121-2015, 2015

von Glasow, R., von Kuhlmann, R., Lawrence, M. G., Platt, U., Crutzen, P. J.: Impact of reactive bromine chemistry in the troposphere, Atmos. Chem. Phys., 4, 2481–2497, 2004

Wang, Y., Jacob, D.J., and Logan, J.A.: Global simulation of tropospheric O_3-NO_x-hydrocarbon chemistry 1. Model formulation, J. Geophys. Res., 103, 10713–10725, doi:10.1029/98jd00158, 1998

Wang, Q., Jacob, D.J., Fisher, J.A., Mao, J., Leibensperger, E.M., Carouge, C.C., Le Sager, P., Kondo, Y., Jimenez, J.L., Cubison, M.J., and Doherty, S.J.: Sources of carbonaceous aerosols and deposited black carbon in the Arctic in winter-spring: implications for radiative forcing, Atmos. Chem. Phys., 11, 23, 12453-12473, doi:10.5194/acp-11-12453-2011, 2011

Wang, S.-Y., Schmidtd, J., Baidar, S., Coburn, S., Dix, B., Koenig, T., Apel, E., Bowdalo, D., Campos, T., Eloranta, E., Evans, M., DiGangii, J., Zondlo, M., Gao, R.-S., Haggerty, J., Hall, S., Hornbrook, R., Jacob, D., Morley, B., Pierce, B., Reeves, M., Romashkin, P., ter Schure, A., and Volkamer, R.: Active and widespread halogen chemistry in the tropical and subtropical free troposphere, P. Natl. Acad. Sci. USA, 112, 9281–9286, doi:10.1073/pnas.1505142112, 2015

Wesely, M.L.: Parameterization of surface resistance to gaseous dry deposition in regional-scale numerical models, Atmos. Environ., 23, 1293–1304, 1989

Whalley, L. K., Furneaux, K. L., Gravestock, T., Atkinson, H. M., Bale, C. S. E., Ingham, T., Bloss, W. J., Heard, D. E.: Detection of iodine monoxide radicals in the marine boundary layer using laser induced fluorescence spectroscopy, J. Atmos. Chem., 58(1), 19–39, 2007

Whalley, L.K., Furneaux, K.L., Goddard, A., Lee, J.D., Mahajan, A., Oetjen, H., Read, K.A., Kaaden, N., Carpenter, L.J., Lewis, A.C., Plane, J.M.C., Saltzman, E.S., Wiedensohler, A., Heard, D.E.: The chemistry of OH

and HO_2 radicals in the boundary layer over the tropical Atlantic Ocean, Atmos. Chem. Phys., 10, 1555-1576, 2010

Whalley, L.K., Blitz, M.A., Desservettaz, M., Seakins, P.W., and Heard, D.E.: Reporting the sensitivity of laser-induced fluorescence instruments used for HO_2 detection to an interference from RO_2 radicals and introducing a novel approach that enables HO_2 and certain RO_2 types to be selectively measured, Atmos. Meas. Tech., 6, 3425-3440, 2013, doi:10.5194/amt-6-3425-2013

Wild, O., Zhu, X., and Prather, M.J.: Fast-J: Accurate Simulation of In- and Below-Cloud Photolysis in Tropospheric Chemical Models, J. Atmos. Chem., 37, 245–282, doi:10.1023/a:1006415919030, 2000

Yan, C., Kocevska, S., and Krasnoperov, L.N.: Kinetics of the reaction of CH_3O_2 radicals with OH studied over the 292-526 K temperature range, J. Phys. Chem. A, 120, 6111-6121, 2016

Yang, X., Cox, R. A., Warwick, N. J., Pyle, J. A., Carver, G. D., O'Connor, F. M., Savage, N. H.: Tropospheric bromine chemistry and its impacts on ozone: A model study, J. Geophys. Res., 110, D23311, doi:10.1029/2005JD006244, 2005

Zhang, L., Jacob, D.J., Liu, X., Logan, J.A., Chance, K., Eldering, A., and Bojkov, B.R.: Intercomparison methods for satellite measurements of atmospheric composition: application to tropospheric ozone from TES and OMI, Atmos. Chem. Phys., 10, 4725–4739, doi:10.5194/acp-10-4725-2010, 2010

073 **Figures**

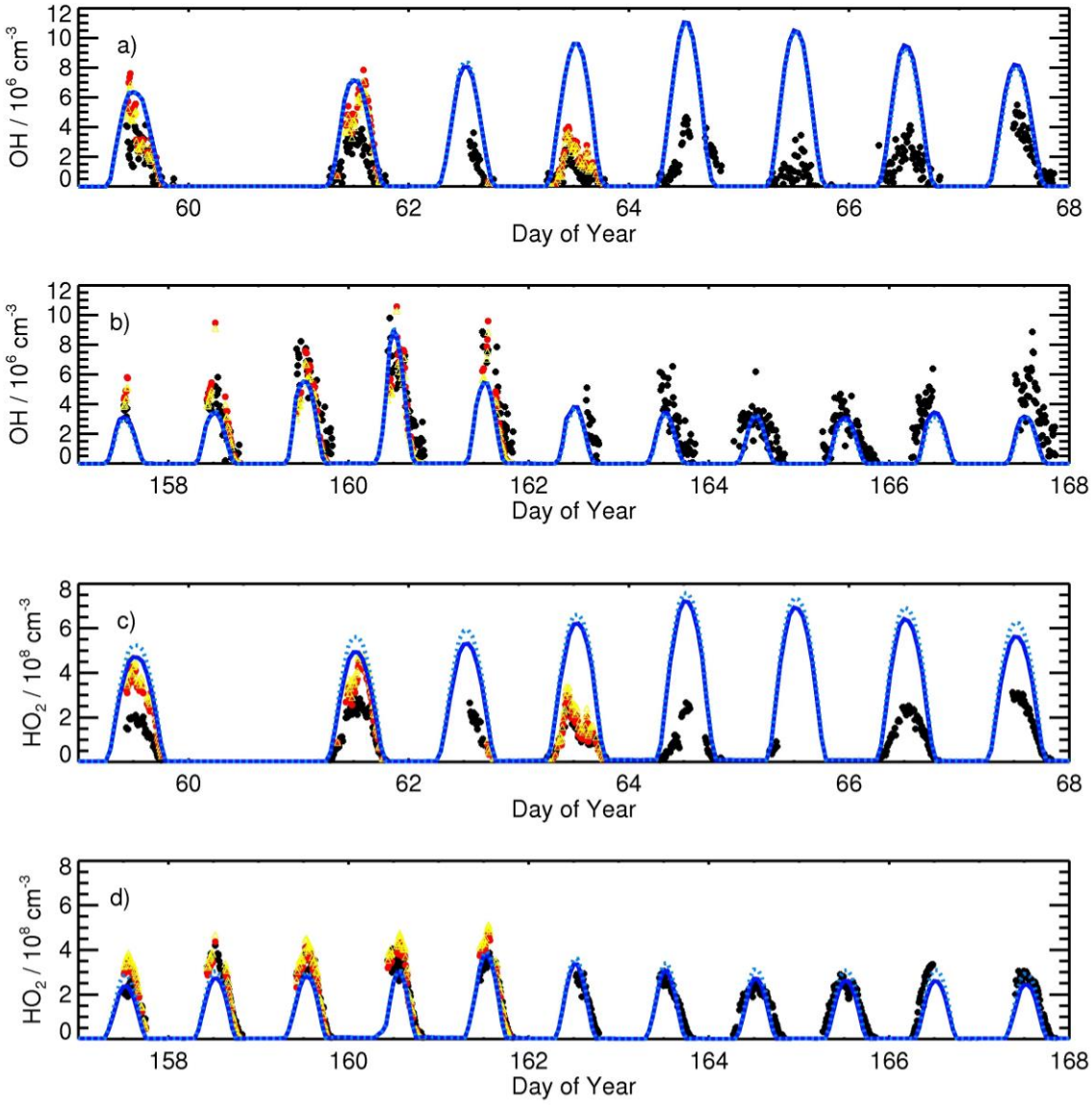

074

075

076 Figure 1: Observed and modelled concentrations of a) OH during SOS1 (February-March 2009, days 58-68); b)
077 OH during SOS2 (May-June 2009, days 157-168); c) HO_2 during SOS1; d) HO_2 during SOS2. Observed data are
078 shown in black; box model concentrations with halogen chemistry are shown by filled red circles; box model
079 concentrations without halogen chemistry are shown by open yellow triangles; global model concentrations with
080 halogen chemistry are shown by solid dark blue lines; global model concentrations without halogen chemistry
081 are shown by broken blue lines.

082

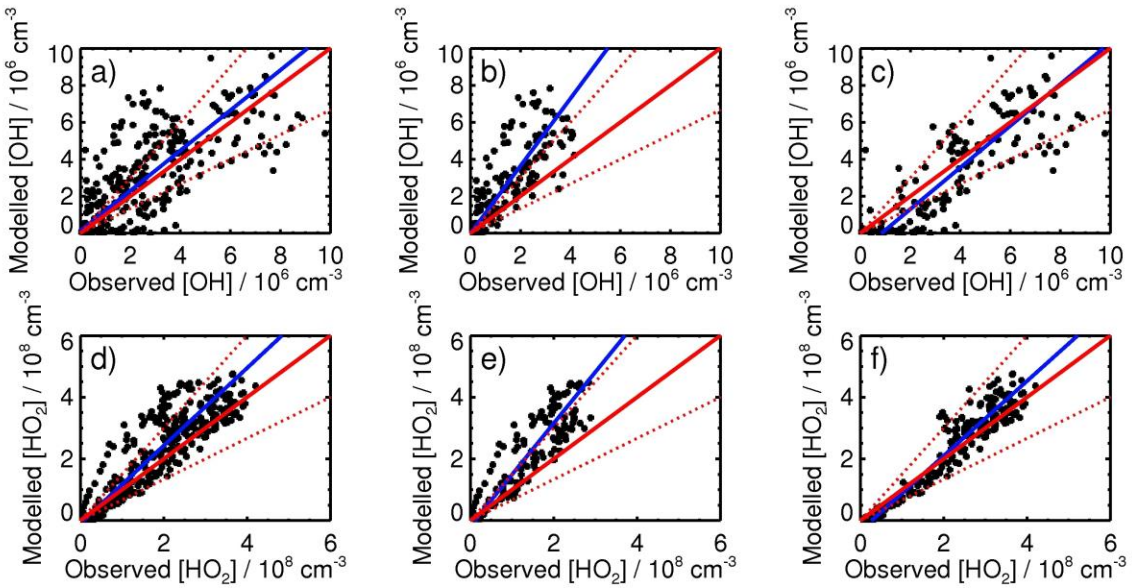

Figure 2: Comparison of modelled and observed concentrations of a) OH during SOS1 (February-March 2009) and SOS2 (May-June 2009); b) OH during SOS1; c) OH during SOS2; d) HO_2 during SOS1 and SOS2; e) HO_2 during SOS1; f) HO_2 during SOS2. In each plot, the solid red line indicates the 1:1 line, with 50 % limits given by the broken red lines. The best fit lines are shown in blue and are described by a) $[OH]_{mod} = (1.09 \pm 0.11) \times [OH]_{obs} + (0.13 \pm 0.38) \times 10^6$ ($r^2 = 0.49$); b) $[OH]_{mod} = (1.82 \pm 0.26) \times [OH]_{obs} - (0.01 \pm 0.51) \times 10^6$ ($r^2 = 0.56$); c) $[OH]_{mod} = (1.11 \pm 0.15) \times [OH]_{obs} - (0.95 \pm 0.66) \times 10^6$ ($r^2 = 0.64$); d) $[HO_2]_{mod} = (1.26 \pm 0.10) \times [HO_2]_{obs} - (0.08 \pm 0.22) \times 10^8$ ($r^2 = 0.77$); e) $[HO_2]_{mod} = (1.66 \pm 0.21) \times [HO_2]_{obs} - (0.17 \pm 0.34) \times 10^8$ ($r^2 = 0.78$); f) $[HO_2]_{mod} = (1.21 \pm 0.12) \times [HO_2]_{obs} - (0.32 \pm 0.30) \times 10^8$ ($r^2 = 0.91$).

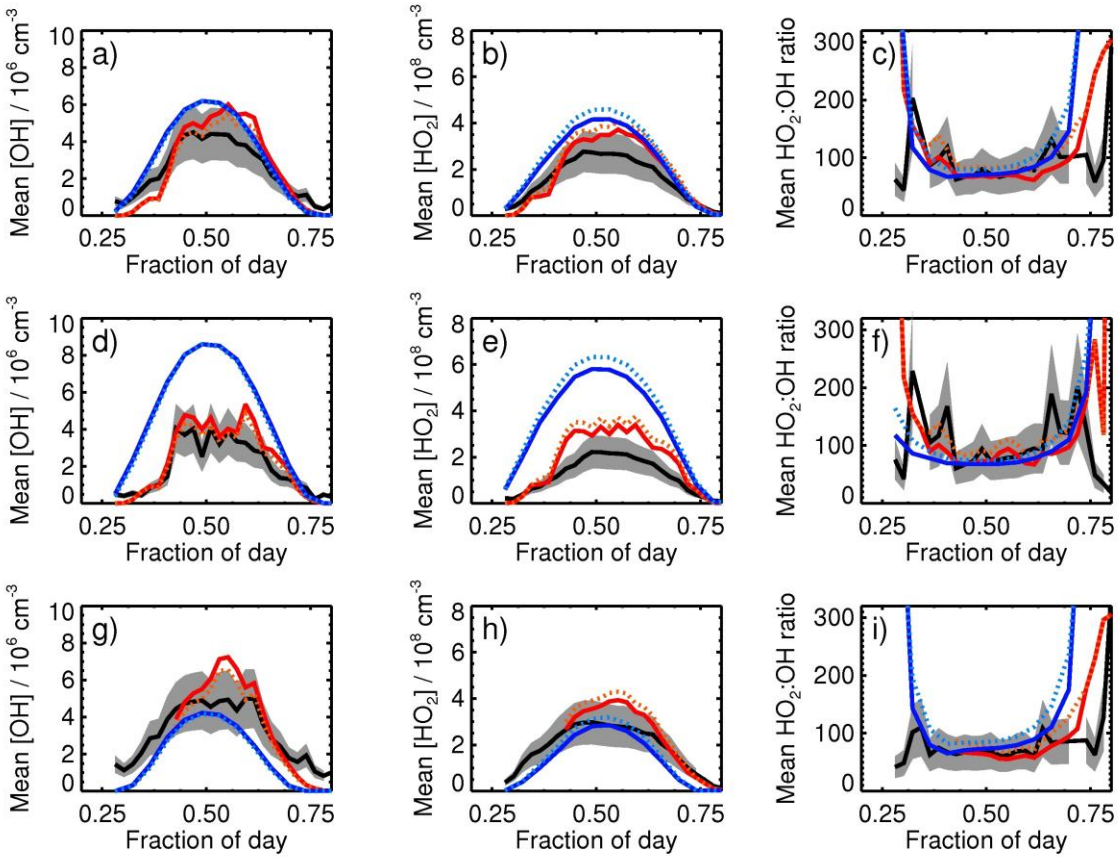

Figure 3: Average diurnal profiles during the Seasonal Oxidant Study (SOS) at the Cape Verde Atmospheric Observatory for a) OH during both measurement periods; b) HO_2 during both measurement periods; c) HO_2:OH ratio during both measurement periods; d) OH during SOS1 (Feb-Mar 2009); e) HO_2 during SOS1; f) HO_2:OH during SOS1; g) OH during SOS2 (May-June); h) HO_2 during SOS2; i) HO_2:OH ratio during SOS2. Observed data are shown in black, with grey shading indicating the variability in the observations; box model output with halogen chemistry is shown by solid red lines; box model output without halogen chemistry is shown by broken orange lines; global model output with halogen chemistry is shown by solid dark blue lines; global model output without halogen chemistry is shown by broken blue lines.

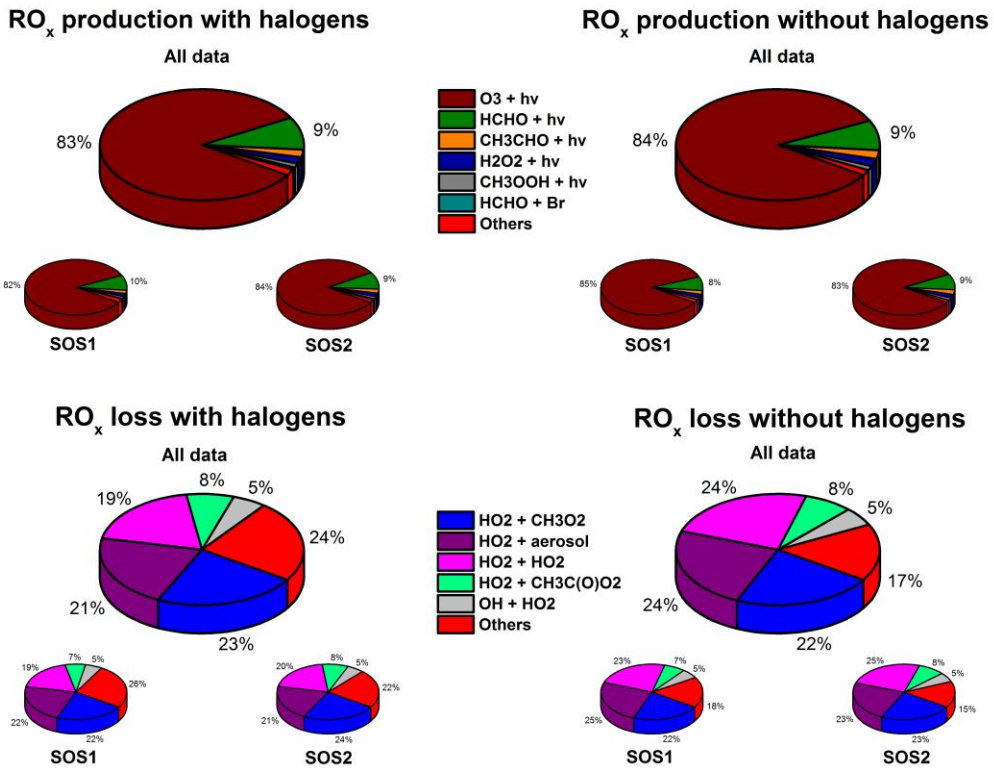

Figure 4: Processes controlling the a) instantaneous RO_x radical production (with RO_x defined here as $OH+HO_2+HOBr+HOI+RO+RO_2$ owing to the rapid processing between HO_2 and HOBr/HOI) around noon (1100-1300 hours) for box model simulations with halogen chemistry; b) the instantaneous RO_x radical production around noon for box model simulations without halogen chemistry; c) the instantaneous RO_x radical loss around noon for box model simulations with halogen chemistry; d) the instantaneous RO_x radical loss around noon for box model simulations without halogen chemistry. The main charts show the average results for SOS1+SOS2, with results for SOS1 and SOS2 shown separately in the inset charts.

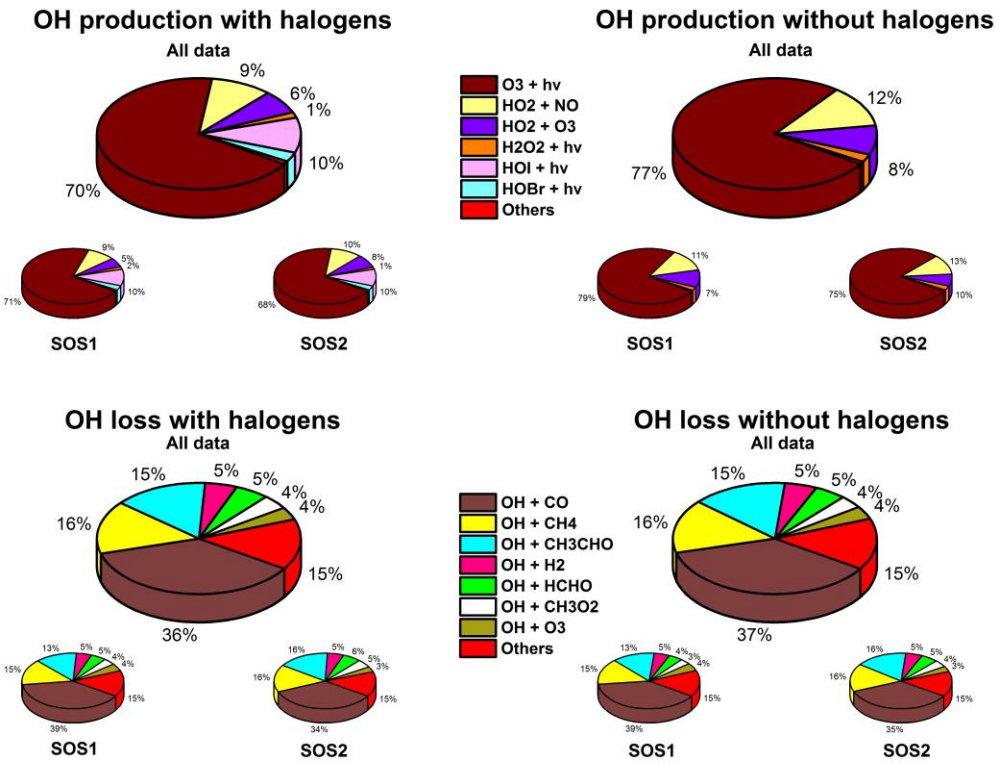

Figure 5: Processes controlling the a) instantaneous OH radical production around noon (1100-1300 hours) for box model simulations with halogen chemistry; b) the instantaneous OH radical production around noon for box model simulations without halogen chemistry; c) the instantaneous OH radical loss around noon for box model simulations with halogen chemistry; d) the instantaneous OH radical loss around noon for box model simulations without halogen chemistry. The main charts show the average results for SOS1+SOS2, with results for SOS1 and SOS2 shown separately in the inset charts.

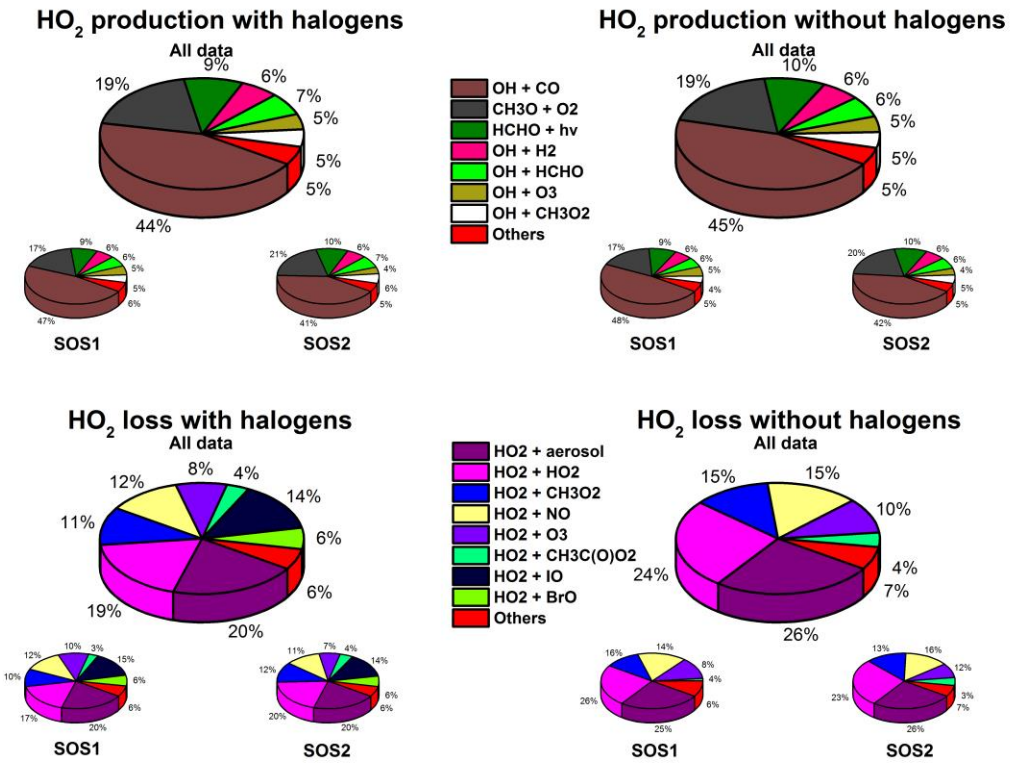

Figure 6: Processes controlling the a) instantaneous HO_2 radical production around noon (1100-1300 hours) for box model simulations with halogen chemistry; b) the instantaneous HO_2 radical production around noon for box model simulations without halogen chemistry; c) the instantaneous HO_2 radical loss around noon for box model simulations with halogen chemistry; d) the instantaneous HO_2 radical loss around noon for box model simulations without halogen chemistry. The main charts show the average results for SOS1+SOS2, with results for SOS1 and SOS2 shown separately in the inset charts.

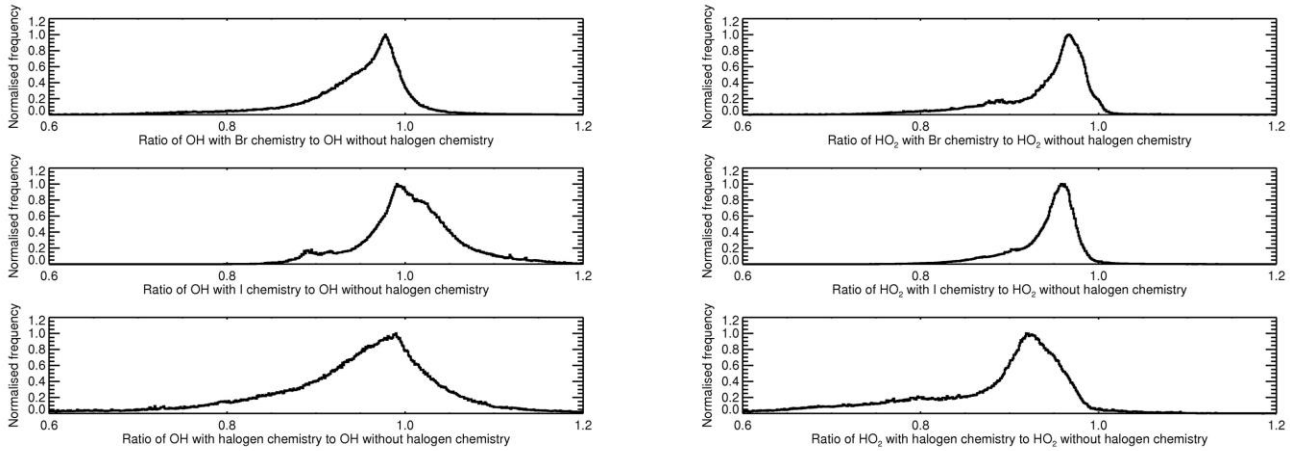

Figure 7: Normalised probability distribution functions showing the fractional changes in OH (left hand side) and HO_2 (right hand side) in GEOS-Chem for all grid boxes on inclusion of bromine chemistry (upper panels), iodine chemistry (middle panels) and bromine and iodine chemistry combined (lower panels).

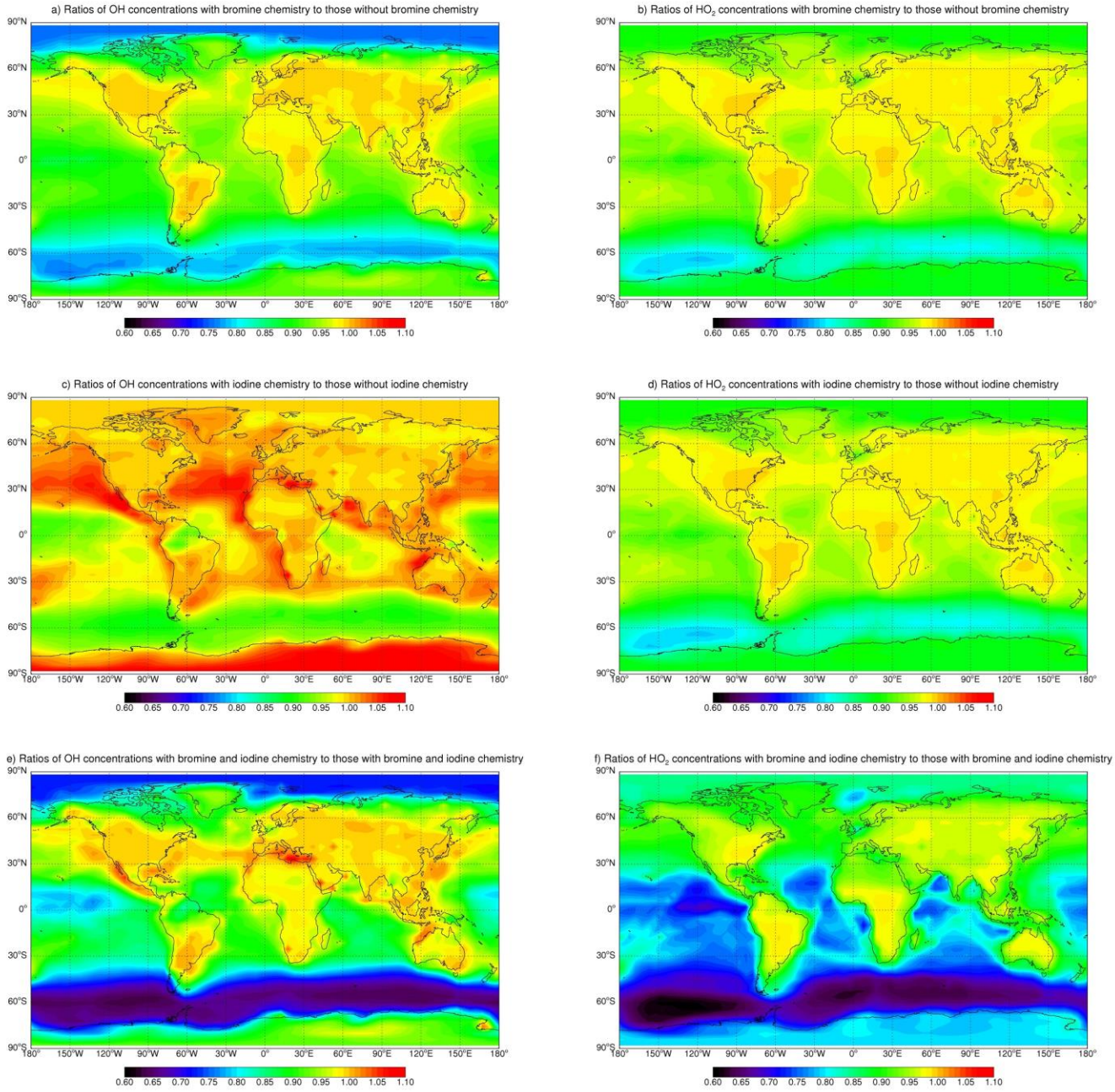

132

133 Figure 8: Percentage changes to annual surface layer concentrations of OH (left hand side) and HO_2 (right hand
134 side) in GEOS-Chem on inclusion of bromine chemistry (upper panels), iodine chemistry (middle panels) and
135 bromine and iodine chemistry combined (lower panels).

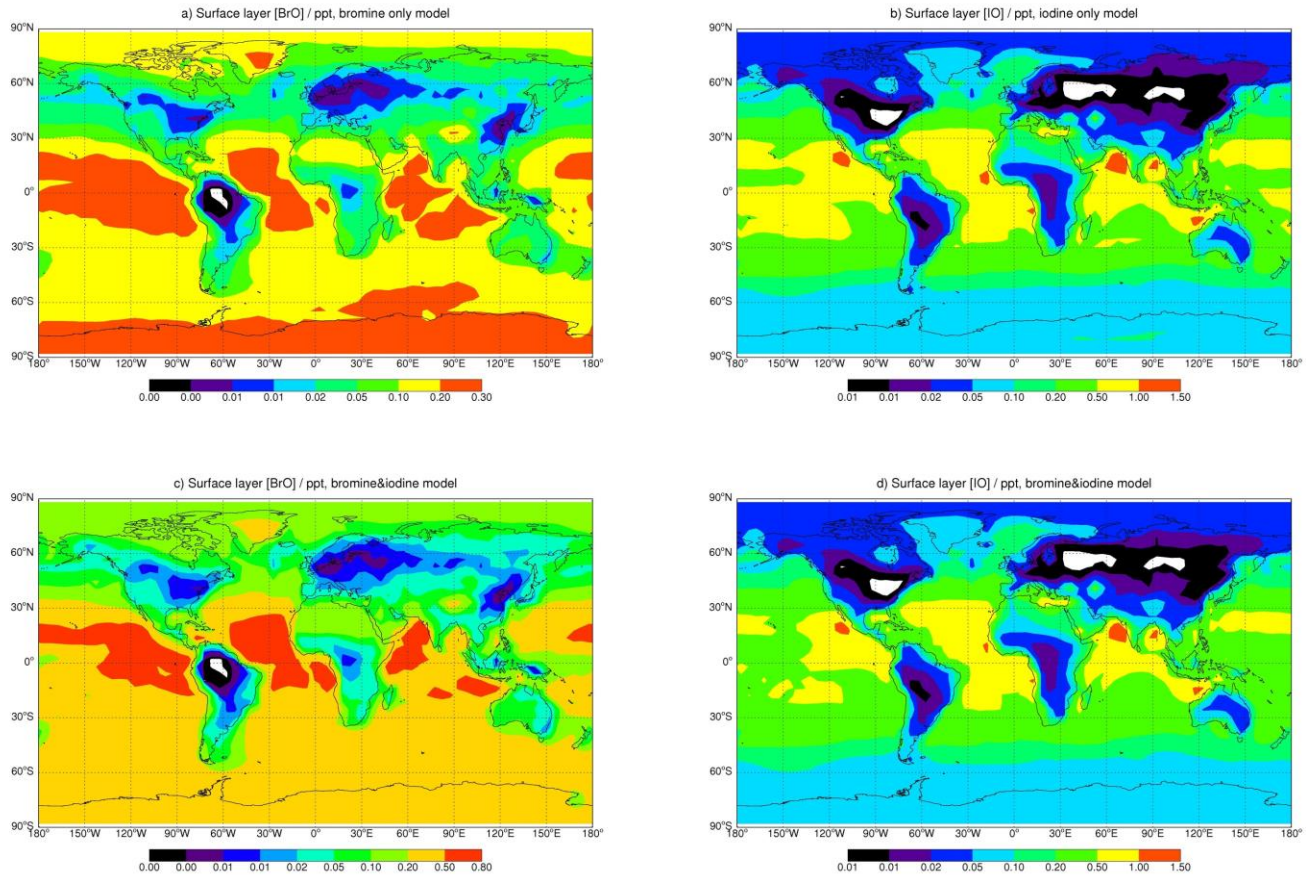

Figure 9: Annual surface layer mixing ratios (ppt) of BrO and IO radicals in GEOS-Chem for model runs with just bromine chemistry (upper left panel), just iodine chemistry (upper right panel) and bromine and iodine chemistry combined (lower panels)